UNIVERSITY OF KASDI MERBAH - OUARGLA
FACUTLY OF MATHEMATICS AND MATTER SCIENCES
DEPARTMENT OF PHYSICS

Order N °:
Serial N °:

A Master Thesis

Submitted by

Nadjah Khemgani

In Fulfillment of the Requirements for the Degree of Master in

Theoretical Physics

Properties of a Reissner-Nordström Black Hole immersed in Dark Matter Perfect fluid

---

Publicaly defended in front of the jury members:

President	Khodja Lamine	Prof.	Univ. KASDI MERBAH OUARGLA
Supervisor	Trad Houssameddine	Prof.	Univ. KASDI MERBAH OUARGLA
Examiner	Belghitar Elhadj	Prof.	Univ. KASDI MERBAH OUARGLA

Academic year: 2025/2026

dedication

I dedicate this work to myself.
To the old version of me who endured a lot, to the current version who did not give up despite all the difficulties to the future version who still chases her dreams with confidence and hope.
To my dear parents, who have always been a source of strength, support, and prayers.
To whom I owe all my love, gratitude, and appreciation for everything they have done for me.
And to everyone who tried to achieve their dream despite fatigue, circumstances, and obstacles.
To those who believed that the difficult path could lead To the most beautiful successes, this work is also dedicated to you.

ACKNOWLEDGMENTS

Praise be to Allah, first and last, for His blessings and guidance, which granted me the strength and patience to complete this work.
I extend my heartfelt thanks and appreciation to my dear parents, who have been my support and constant encouragement throughout my academic journey. Thanks to their prayers and continuous encouragement, I have been able to reach this stage.
I would also like to extend my heartfelt thanks and gratitude to everyone who contributed to my assistance and guidance, and to my esteemed professors for the knowledge, advice, and guidance they provided.
And thank you to the old Nadjah, the present Nadjah, and the future Nadjah.
In conclusion, I thank everyone who stood by me and contributed, directly or indirectly, to the completion of this thesis.

الملخص

تتناول هذه المذكرة دراسة بنية الزمكان في إطار النسبية العامة، مع التركيز بشكل خاص على الثقب الأسود المشحون من نوع ريزنر–نوردستروم المغمور في مادة مظلمة من نوع المائع المثالي.
تبدأ الدراسة بعرض المبادئ الأساسية للنسبية الخاصة والعامة، مع تقديم معادلات أينشتاين التي تصف تأثير المادة والطاقة على انحناء الزمكان، إضافة إلى التطرق إلى الحلول ذات التناظر الكروي كأساس لبناء مقاييس الثقوب السوداء.
يتم في الجزء الأساسي اشتقاق مقياس ريزنر–نوردستروم انطلاقًا من معادلات أينشتاين–ماكسويل التي تأخذ بعين الاعتبار تأثير كل من الكتلة والشحنة الكهربائية على هندسة الزمكان .بعد ذلك يتم تعميم هذا الحل بإدخال تأثير المادة المظلمة، حيث يؤدي ذلك إلى تعديل عنصر المترية بإضافة حد لوغاريتمي يعكس تأثير الحقل المظلم على البنية الهندسية للزمكان.
كما يتم تحليل الخصائص الفيزيائية للنموذج الناتج، وخاصة بنية أفق الحدث وتأثير المادة المظلمة على موقعه واستقراره .بالإضافة إلى ذلك، تتم دراسة حركة الجسيمات في هذا الزمكان، مع اشتقاق شروط المدارات الدائرية وتحديد نصف قطر المدار الدائري المستقر الداخلي.
تُظهر النتائج أن إدخال المادة المظلمة PFDM يؤدي إلى تعديلات مهمة على بنية الزمكان، ويؤثر بشكل مباشر على خصائص الثقب الأسود المشحون مقارنة بالحالة التقليدية لريزنر–نوردستروم.

الكلمات المفتاحية:
النسبية العامة، ثقب ريزنر–نوردستروم، مادة مظلمة سائلة مثالية (PFDM)

Résumé

Cette mémoire étudie la structure de l’espace-temps dans le cadre de la relativité générale, en se concentrant particulièrement sur le trou noir chargé de type Reissner–Nordström immergé dans de la matière noire sous forme de fluide parfait (PFDM).
L’étude commence par la présentation des principes fondamentaux de la relativité restreinte et générale, ainsi que des équations d’Einstein décrivant l’influence de la matière et de l’énergie sur la courbure de l’espace-temps. Elle aborde également les solutions à symétrie sphérique comme base pour la construction des métriques des trous noirs.
La partie principale consiste à dériver la métrique de Reissner–Nordström à partir des équations d’Einstein–Maxwell, qui prennent en compte les effets de la masse et de la charge électrique sur la géométrie de l’espace-temps. Cette solution est ensuite généralisée en introduisant l’effet de la matière noire de type PFDM, ce qui conduit à une modification de la métrique par l’ajout d’un terme logarithmique représentant l’influence du champ sombre sur la structure de l’espace-temps.
Les propriétés physiques du modèle obtenu sont ensuite analysées, notamment la structure de l’horizon des événements ainsi que l’impact de la matière noire sur sa position et sa stabilité. En outre, le mouvement des particules dans cet espace-temps est étudié, avec la dérivation des conditions des orbites circulaires et la détermination du rayon de l’orbite circulaire stable interne (ISCO).

Les résultats montrent que l’introduction de la matière noire PFDM entraîne des modifications importantes de la structure de l’espace-temps et affecte directement les propriétés du trou noir chargé par rapport au cas classique de Reissner–Nordström.

Mots-clés :
Relativité Générale, Trou Noir Reissner–Nordström, Matière Noire à Fluide Parfait (PFDM)

Abstract

This memorandum addresses the study of spacetime structure within the framework of general relativity, with a particular focus on the charged Reissner–Nordström black hole immersed in a dark matter of the ideal fluid type.

This memorandum focuses on the study of the structure of spacetime within the framework of general relativity, paying particular attention to the charged Reissner–Nordström black hole immersed in ideal dark matter.

The study begins by presenting the fundamental principles of special and general relativity, along with Einstein equations that describe the effect of matter and energy on the curvature of spacetime, in addition to addressing spherically symmetric solutions as the basis for constructing black hole metrics.

The study begins with an introduction to the fundamental principles of special and general relativity, including Einstein equations which describe the effect of matter and energy on the curvature of spacetime. It also covers spherically symmetric solutions as a basis for constructing black hole metrics.

In the main part, the Reissner–Nordström metric is derived from the Einstein–Maxwell equations, which take into account the effects of both mass and electric charge on the geometry of spacetime. Then, this solution is generalized by introducing the effect of dark matter, which leads to modifying the metric component by adding a logarithmic term that reflects the influence of the dark field on the geometric structure of spacetime.

The main part derives the Reissner–Nordström metric from the Einstein–Maxwell equations, which consider the effects of mass and electric charge on the geometry of spacetime. This solution is then generalised by introducing the effect of dark matter, which modifies the metric component by adding a logarithmic term that reflects the dark field's influence on the geometric structure of spacetime.

The physical properties of the resulting model are also analyzed, particularly the structure of the event horizon and the effect of dark matter on its position and stability. Additionally, the motion of particles in this spacetime is studied, deriving the conditions for circular orbits and determining the radius of the stable inner circular orbit.

The resulting model physical properties are analysed, with a particular focus on the structure of the event horizon and the effect of dark matter on its position and stability. Additionally, the motion of particles in this spacetime is studied to derive the conditions for circular orbits and determine the radius of the stable inner circular orbit.

The results show that the introduction of PFDM dark matter leads to significant modifications in the spacetime structure and directly affects the properties of the charged black hole compared to the traditional Reissner–Nordström case.

The results show that introducing PFDM dark matter significantly modifies the structure of spacetime and directly affects the properties of charged black holes, compared to the traditional Reissner–Nordström case.

Keywords:
General Relativity, Reissner–Nordström Black Hole, Perfect Fluid Dark Matter (PFDM).

Contents

The symbols	There meaning
$\gamma = \left(1 - \frac{v^2}{c^2}\right)^{-1/2}$	the Lorentz factor
C	the speed of light
Δs^2	The spacetime interval
E	Energy
$R_{\mu\nu}$	the Ricci tensor
R	the Ricci scalar
$g_{\mu\nu}$	the metric tensor
$T_{\mu\nu}$	the stress-energy tensor
$G_{\mu\nu}$	the Einstein tensor
$\Gamma^{\alpha}_{\mu\beta}$	the Christoffel symbols
K	the Kretschmann scalar
M	mass
J	angular momentum
Q	electric charge
ρ	the energy density
p	the pressure
ξ^{μ}, ψ^{μ}	Killing vectors

INTRODUCTION

I have always been very passionate about the nature of black holes that I heard about in my childhood cartoons, where they seemed to me like mysterious objects that swallow everything that approaches them without anything escaping, as if they were doors to the unknown in the universe. As time passed, this childish perception was no longer enough to satisfy my curiosity, it transformed into a genuine desire to understand this phenomenon from a precise scientific perspective, far removed from the simplistic imaginary image.

My interest has increasingly focused on how black holes form from the collapse of massive stars and on the geometric structure of spacetime around them as described by general relativity and how their intense gravity can distort light and cosmic paths to the extent that no signal can escape the event horizon. My curiosity has also increased regarding the concepts associated with them, such as central singularity and the nature of physical laws under those extreme conditions, where our traditional understanding of time and space collapses.

Albert Einstein presented the clear formulation of the theory of special relativity in 1905, based on the non-Newtonian nature of light and the principle of relativity, with the definition of relative physical quantities, which allowed for a reconstruction of our understanding of time, space, and motion within a framework more precise and consistent with modern experiments [1, 2]. This theory comes after a period when Newtonian physics was at its peak by the end of the 19th century, when it was believed that everything in time and space could be predicted accurately if the current state of the system and its laws were known, in accordance with the concept of absolute time and space. However, numerous experiments, most notably the Michelson-Morley experiment in 1887 [3], demonstrated that the speed of light is constant and does not depend on the speed of the source or the observer, a behavior that contradicts Newtonian laws of motion [1]. At that time, scientists tried to explain this phenomenon by modifying the properties of space and introducing the concept of ether, but these explanations were not consistent with the fundamental principles of Newtonian physics [2]. Later, Poincaré recognized the limitations of Newtonian physics in describing electromagnetic phenomena and emphasized the need for new non-classical physical concepts. His insights contributed significantly to the development of the foundations of special relativity.

Despite the remarkable success of special relativity in describing the relationship between time and space and explaining phenomena associated with high speeds, it remained unable to provide a complete description of gravity [4, 5]. In Newtonian mechanics, gravity was interpreted as a force acting instantaneously between masses, an idea that became incompatible with the principles of relativity, especially with the impossibility of transmitting information faster than the speed of light. These contradictions drove Albert Einstein to search for a deeper theory capable of reconciling gravity with the principles of relativity [5, 6].

In 1915, Einstein presented the general theory of relativity, which revolutionized the classical understanding of gravity by describing it not as a traditional force but as a manifestation of the curvature of spacetime resulting from the presence of mass and energy [7, 5]. According to this theory, massive bodies distort the geometric structure of spacetime, and this curvature determines the motion of matter and radiation [4, 6]. Einstein's field equations established the mathematical framework that connects the distribution of matter and energy to the geometry of spacetime itself [7, 9].

One of the most impressive predictions of general relativity was the existence of black holes, which are extremely dense astronomical bodies whose gravitational fields become so strong that nothing, not even light, can escape from them beyond a boundary known as the event horizon [10, 6]. These solutions naturally emerged from Einstein's equations through the work of Karl Schwarzschild and later through more general solutions like the Reissner-Nordström (RN) metric, which describes charged black holes [7, 10]. The study of these objects has become one of the most important fields in modern gravitational physics due to their deep connection with spacetime geometry, singularities, and extreme gravitational phenomena [10].

After the development of general relativity, black holes emerged as one of the most interesting predictions in Einstein's theory of gravity. These compact objects form when a star with a sufficiently large mass collapses under the influence of gravity at the end of its life cycle, causing the concentration of matter within an extremely small region of spacetime [6]. The resulting gravitational field becomes so strong that nothing can escape once it crosses the event horizon.

In general, the characterization of black holes through only a few physical quantities is closely related to the no-hair theorem, which states that stationary black holes can be completely described by a limited set of observable parameters: mass, electric charge, and angular momentum. According to this theory, all other details related to the matter that originally formed the black hole are lost from external observation after the gravitational collapse. Black holes can be classified according to their basic physical properties. The simplest type is the Schwarzschild black hole, which is characterized only by its mass and represents a static, uncharged solution to the Einstein field equations [6]. The more general solutions include the RN black hole, which is characterized by both mass and electric charge, and the Kerr black hole, which possesses angular momentum and describes the rotating spacetime geometry. The most complete classical solution is the Kerr-Newman black hole, which simultaneously features mass, electric charge, and rotation [10].

In parallel with the study of black holes, recent cosmic observations have revealed another major mystery in the universe known as dark matter [12, 13]. Astronomical evidence such as galaxy rotation curves, gravitational lensing, and large-scale structure formation indicates the presence of an invisible form of matter that interacts gravitationally but does not emit or absorb electromagnetic radiation [12, 18]. Dark matter is believed to constitute a significant portion of the total matter content in the universe and plays a fundamental role in the evolution of cosmic structures. Therefore, studying black holes in the presence of dark matter environments has become an important research trend to understand the potential modifications in spacetime geometry and the behavior of gravitational systems under realistic astronomical conditions [19].

Driven by the importance of understanding the interaction between black holes and dark matter environments, this work focuses on studying the RN black hole surrounded by a perfect fluid dark matter (PFDM) [19, 15]. The presence of PFDM modifies the spacetime geometry around the black hole and provides additional corrections to the gravitational field, leading to significant changes in many physical and engineering properties of the system. These modifications provide an interesting framework for investigating the impact of dark matter on relativistic compact objects and exploring the potential astronomical effects associated with strong gravitational fields [15].

In this context, the current study begins with the formulation of the modified RN metric using PFDM and the deduction of the corresponding spacetime geometry from the Einstein field equations. Special attention is given to the role played by the dark matter parameter in modifying the scale structure and its associated prospects. The derivation highlights how the coupling between the electric charge and the surrounding dark matter medium affects the classical RN solution, leading to a richer gravitational structure [15].

In addition, this study examines the motion of particles around the black hole by analyzing circular orbits and determining the innermost stable circular orbit (r_{ISCO}), which plays a fundamental role in black hole physics and accretion disk physics. Additionally, several important properties of the RN black hole modified by PFDM are examined, including the structure of event horizons and the behavior of spacetime curvature. Through these analyses, the study aims to provide a deeper understanding of the effects of dark matter on charged black holes within the framework of general relativity.

Chapter 1

Special and General Relativity

Special relativity (SR) is a physical theory that describes space and time based on a mathematical model, and it is built on the concept of inertial frames as in Newtonian mechanics. However, the fundamental difference between it and classical physics is the abandonment of the idea of absolute time. This led to the emergence of Lorentz transformations[3], which connect inertial frames moving relative to each other while keeping the speed of light constant in all these frames[4].

General relativity (GR) extends the principles of special relativity to include non-inertial frames and provides a new description of gravity. Based on the principle of equivalence, gravity is explained not as a force but as the curvature of spacetime resulting from mass and energy. This theory successfully explains many physical phenomena, such as the bending of light near massive objects and gravitational time dilation [7]. Together, special and general relativity form a coherent theoretical framework for understanding the deep structure of the universe at both microscopic and cosmological scales.

1.1 Special Relativity

1.1.1 Principles of Special Relativity

Einstein's special theory of relativity is founded on two fundamental postulates.

- The first postulate, known as the principle of relativity, states that the laws of physics are the same in all inertial reference frames. This implies that no physical experiment carried out in a system moving at a constant velocity can reveal whether the system is at rest or in uniform motion, meaning that all inertial observers will describe the same physical phenomena in identical ways.

- The second postulate asserts the constancy of the speed of light in a vacuum: it remains the same for all observers, regardless of the motion of the light source or the observer. This principle leads directly to profound consequences such as time dilation, length contraction, and the relativity of simultaneity, which distinguish special relativity from classical Newtonian mechanics [4].

1.1.2 Lorentz transformations

Any event in an inertial frame can be described by spacetime coordinates (x, y, z, t) defined using universal units of length and time. When passing from inertial frame S to S', it becomes necessary to determine the transformation laws that relate the coordinates of the same event in the two frames [2], that is :

$$(x, y, z, t) \to (x', y', z', t').$$

In special relativity, coordinate transformations help us understand how to describe events from different perspectives of inertial observers. These transformations ensure that the spacetime interval between events remains constant, while maintaining the same physical laws for each observer. It also allows us to express the same event but for a different coordinate frame [5].

$$x' = \gamma(x - vt), \tag{1.1}$$

$$t' = \gamma\left(t - \frac{vx}{c^2}\right), \tag{1.2}$$

$$y' = y, \tag{1.3}$$

$$z' = z. \tag{1.4}$$

Where $\gamma = (1 - \frac{v^2}{c^2})^{-1/2}$,$\gamma$ the Lorentz factor, v the v frame speed S' relative to S, c constant speed (the speed of light in a vacuum). A simple explanation is that x' depends on x and t because the motion is in the direction of x, wile y' and z' do not change because the movement does not affect them. t' it is a change in time due to the extension of time.

1.1.3 Four-dimensional Spacetime (Minkowski Space)

Spacetime Diagrams and World Lines

The spacetime diagram depicts the motion of events and particles clearly, showing the direction of each particle's velocity line and its changes, making it easier to understand the dynamics of motion and the relationships between particles within the framework of special relativity. Figure 1.1 presents a two-dimensional section of spacetime, namely the $t-x$ plane, where the fundamental ideas are illustrated. Each point in this diagram corresponds to a fixed position (x) at a specific time$t$ and is referred to as an (event). A curve in this plane represents a relation of the form $x = x(t)$, and therefore describes the motion of a particle through time. This curve is known as the particle's world line, and its slope is directly related to the particle's velocity [4] given in the statement:

$$\text{slope} = \frac{dt}{dx} = \frac{1}{v}.$$

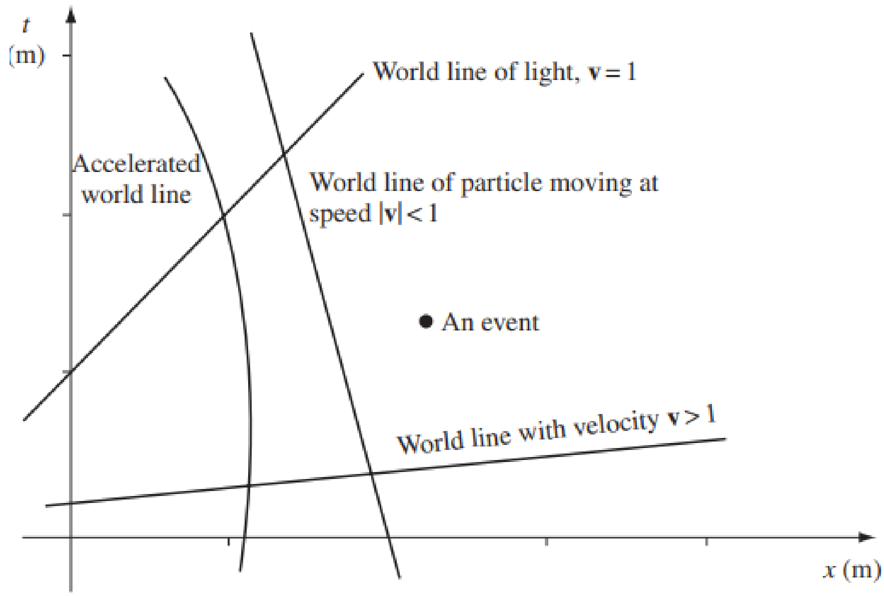

Fig. 1.1 – A spacetime diagram in natural units.

The Spacetime Interval

The spacetime interval is a fundamental quantity in special relativity that combines the spatial and temporal intervals between two events and remains constant for all inertial observers, given by the expression:

$$\Delta s^2 = c^2\Delta t^2 - \Delta x^2 - \Delta y^2 - \Delta z^2, \tag{1.5}$$

where c is the speed of light in vacuum, Δt is the time interval between the two events, $\Delta x, \Delta y, \Delta z$ are the spatial separations between them.

The classification of spacetime intervals is as follows:

- **Timelike** ($\Delta s^2 > 0$): A massive particle can travel between the events, and proper time is measured between them.
- **Spacelike** ($\Delta s^2 < 0$): No object or signal can travel between the events at or below the speed of light; the events can be simultaneous in some inertial frame.
- **Lightlike / Null** ($\Delta s^2 = 0$): Represents the path of light; only light can connect the events [4].

Light Cone

In special relativity, the light cone represents a geometric framework that clarifies which events can causally influence each other within spacetime . For any event P in Minkowski space there exists a unique light cone whose vertex is at P. This cone consists of all directions along which light can travel from P [4]. The light cone divides spacetime into three distinct regions:
Future Light Cone: This region contains all events that can be influenced by the event P ; any signal or object traveling slower than the light from P can reach these events.
Past Light Cone: This region contains all events that could have influenced P; signals or objects

from these events can reach P.
Elsewhere: All other events outside the light cone cannot have a direct causal connection with P, since doing so would require faster-than-light travel.

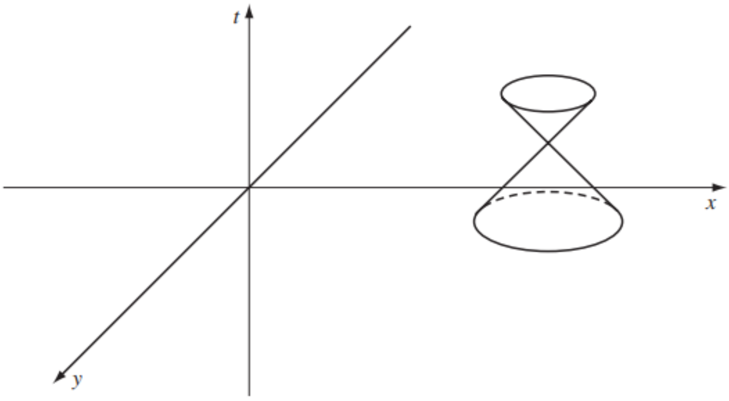

Fig. 1.2 – Light cone.

1.1.4 Results of Special Relativity

Time Dilation

Proper time $\Delta\tau_{AB}$ is defined as the time measured between events A and B by a clock whose worldline passes through both. Time dilation then describes the effect where an observer in relative motion measures a longer duration Δt_{AB} for the same physical interval [4]. More precisely, as the speed of the object approaches the speed of light, the time measured in its own frame becomes shorter than the time measured in a stationary reference frame and the equation is written as follows.

$$\Delta t_{AB} = \gamma\,\Delta\tau_{AB}, \tag{1.6}$$

where $\Delta\tau_{AB}$ the proper time (time measured in the frame of the moving object), Δt the time measured by a stationary observer.

Length Contraction

In two inertial frames, S and S', let a rigid rod of length L_0 be at rest along the x'-axis in S'. When the rod moves relative to S with velocity v, its length measured in S is shorter than L_0. This effect, called length contraction, becomes significant when the speed of the rod approaches the speed of light c [2] ,and the equation is given:

$$L = \frac{L_0}{\gamma}, \tag{1.7}$$

where L the length measured in the frame S, L_0 the rest length, γ the Lorentz factor.

Relativity of Simultaneity

Since each observer provides a coordinate system for spacetime, the axes of a moving observer S' can be drawn on the spacetime diagram of a stationary observer S. The t' axis represents the worldline of S' (constant $x' = 0$), while the x' axis represents events that S' considers simultaneous at $t' = 0$. When mapped onto S's diagram, the x' axis is not parallel to S's x axis, demonstrating that events simultaneous for S' are not simultaneous for S. This geometrical construction, based on the invariance of the speed of light, illustrates the inescapable relativity of simultaneity in special relativity [4].

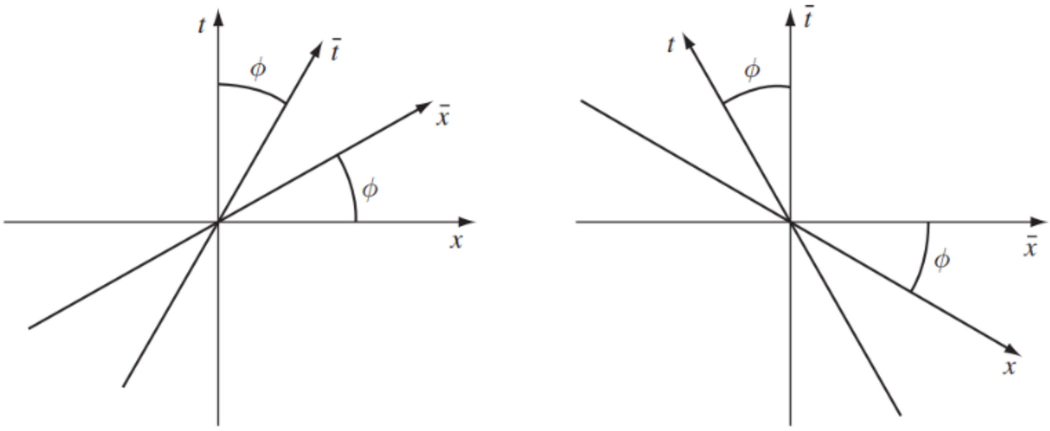

Fig. 1.3 – Spacetime diagrams of S (left) and S' (right) .

Mass-Energy Equivalence

The special theory of relativity demonstrates that classical mechanics is no longer valid when dealing with velocities comparable to the speed of light. Under these conditions, the kinetic energy of a particle cannot be described by the classical formula $K = \frac{1}{2}mv^2$; instead [8], it follows the relativistic expression:

$$E = \gamma mc^2. \tag{1.8}$$

Expanding the relativistic energy for velocities much smaller than c yields:

$$E \approx mc^2 + \frac{1}{2}mv^2 + \cdots \tag{1.9}$$

The first term, mc^2, represents the intrinsic energy associated with the mass of the particle (rest energy). This result leads to the unification of the conservation laws of mass and energy, showing that mass and energy are equivalent and can be transformed into each other according to the relation:

$$E = mc^2. \tag{1.10}$$

1.2 General Relativity

Before the development of General relativity, classical notions of space and time dominated physics. The advent of special relativity redefined the structure of spacetime, revealing that Newtonian gravity, which assumes instantaneous action at a distance, is inconsistent with this framework. Motivated by the need for a theory compatible with the relativistic structure of spacetime, Einstein developed general relativity. This theory extends the concepts of special relativity to include gravity, describing it not as a force but as the curvature of spacetime caused by mass and energy. The motion of freely falling bodies follows geodesics in this curved spacetime [7], and the relationship between matter and spacetime geometry is formalized in Einstein's field equations:

$$R_{\mu\nu} - \frac{1}{2}Rg_{\mu\nu} = \frac{8\pi G}{c^4}T_{\mu\nu}. \tag{1.11}$$

where $G_{\mu\nu}$ the Einstein tensor describing the curvature of spacetime, Λ the cosmological constant, $T_{\mu\nu}$ is the stress-energy-momentum tensor of matter, G is the gravitational constant, c the speed of light, and $g_{\mu\nu}$ the metric tensor.

1.2.1 Principles of General Relativity

Equivalence Principle

The principle of equivalence, which is fundamental to general relativity, arises from the observation that gravitational and inertial mass are equal $m_{inert} = m_{grav}$. This can be illustrated by Einstein's thought experiment of an elevator in empty space. If the chest is accelerated upwards by a rope, an observer inside feels a force pressing him to the floor, just as he would experience in a gravitational field. Objects released inside the elevator accelerate towards the floor at the same rate, regardless of their mass. From the observer's perspective, it is impossible to distinguish between acceleration and gravity. This equivalence

$$F_g = m_{\text{grav}}\, g = m_{\text{inert}}\, a \;\Rightarrow\; a = \frac{m_{\text{grav}}}{m_{\text{inert}}}\, g \;\Rightarrow\; a = g. \tag{1.12}$$

Between acceleration and gravitational effects forms the core of the equivalence principle, providing the foundation for general relativity and the idea that gravity can be understood as a manifestation of spacetime curvature rather than a conventional force [8].

General Covariance

In special relativity, the laws of nature are assumed to have the same form in all inertial reference frames, i.e., frames moving at constant speed along straight lines, where free particles move in straight lines at constant velocity and the mechanical and optical laws take their simplest form. However, when considering accelerated or non-uniformly moving frames, noticeable differences appear in the behavior of objects, as illustrated by the example of a moving railway carriage with sudden braking, where the occupant feels a force due to the acceleration. This shows that the principle of special relativity is limited to inertial frames and cannot be directly applied to all states of motion. From this observation arises the need to formulate the laws of nature so that they remain valid in any reference frame, regardless of its state of motion, which leads to the concept of general covariance. This generalization requires formulating the laws in a geometric way, independent of coordinates, so that matter and energy determine the curvature of spacetime and particles move along geodesics, without reliance on any specific reference frame. Through this progression, one moves from the principle of special relativity to the principle of generalization, which forms the foundation of general relativity and its geometric formulation of physical laws [8].

1.2.2 Einstein's Equations

General relativity describes gravity not as a force, but as the curvature of spacetime resulting from the presence of matter and energy. The fundamental equations of this theory, known as

Einstein's field equations, relate the geometry of spacetime to the energy and momentum of the matter contained within it. The field equations are given by:

$$R_{\mu\nu} - \frac{1}{2} R\, g_{\mu\nu} = \frac{8\pi G}{c^4} T_{\mu\nu}, \tag{1.13}$$

where

- $R_{\mu\nu}$ is the Ricci tensor is obtained by contracting the Riemann curvature tensor [16].

$$R^{\rho}{}_{\sigma\mu\nu} = \partial_\mu \Gamma^{\rho}_{\nu\sigma} - \partial_\nu \Gamma^{\rho}_{\mu\sigma} + \Gamma^{\rho}_{\mu\lambda}\Gamma^{\lambda}_{\nu\sigma} - \Gamma^{\rho}_{\nu\lambda}\Gamma^{\lambda}_{\mu\sigma}, \tag{1.14}$$

$$\Rightarrow R_{\mu\nu} = R^{\lambda}{}_{\mu\lambda\nu}. \tag{1.15}$$

  It represents the part of spacetime curvature that is directly influenced by the presence of matter. Physically, it describes how nearby geodesics converge or diverge, indicating the effect of gravity on the motion of particles.

- R is the Ricci scalar, a trace of $R_{\mu\nu}$ summarizing overall curvature.

$$R = g^{\mu\nu} R_{\mu\nu}. \tag{1.16}$$

  It provides a scalar measure of curvature, summarizing the overall geometric deformation of spacetime at a point. Unlike $R_{\mu\nu}$, it does not carry directional information.

- $g_{\mu\nu}$ is the metric tensor, defining distances and angles in spacetime and is given by:

$$ds^2 = g_{\mu\nu} dx^\mu dx^\nu. \tag{1.17}$$

- $T_{\mu\nu}$ is the stress-energy tensor, describing the density and flux of energy and momentum,For example, in the case of a perfect fluid:

$$T_{\mu\nu} = (\rho + p) u_\mu u_\nu + p g_{\mu\nu}, \tag{1.18}$$

  where ρ is the energy density, p is the pressure, and u^μ is the four-velocity. This tensor acts as the source of spacetime curvature.

- The gravitational constant G determines the strength of gravity, while the speed of light c ensures consistency with relativity. The coupling factor in Einstein's field equations is:

$$\frac{8\pi G}{c^4}.$$

  This factor ensures that, in the weak-field limit, the equations reduce to Newtonian gravity. This equation shows that spacetime geometry (left-hand side) is determined by the distribution of matter and energy (right-hand side).

In vacuum, where no matter is present, the equations reduce to:

$$R_{\mu\nu} = 0 \tag{1.19}$$

This simplification is used to describe solutions such as black holes, where spacetime curvature exists even without matter. In essence, Einstein's equations tell us that matter tells spacetime how to curve, and curved spacetime tells matter how to move [5].

1.2.3 killing vector

In general relativity, the geometry of spacetime is completely described by the metric tensor $g_{\mu\nu}$, which encodes the gravitational field and determines the motion of particles and light. The metric defines the spacetime interval (1.17). and plays a central role in formulating the laws of physics in curved spacetime.
An essential feature of any spacetime is the presence of symmetries. These symmetries are not merely mathematical in nature; they carry significant physical implications, especially in the analysis of geodesic motion. In particular, symmetries of the metric often give rise to conserved quantities along the trajectories of freely moving particles. To express these symmetries in a fully coordinate-independent (covariant) manner, one introduces the concept of Killing vector fields.
A Killing vector field K^μ is defined as a vector field that generates an isometry of the spacetime, meaning that the metric remains invariant along its flow. This condition is expressed mathematically by Killing's equation:

$$\nabla_\mu K_\nu + \nabla_\nu K_\mu = 0.$$

The importance of Killing vectors lies in their direct connection to conserved quantities. For a particle moving along a geodesic with four-momentum p^μ, the scalar quantity:

$$K_\mu p^\mu,$$

is conserved along the trajectory:

$$\frac{d}{d\lambda}(K_\mu p^\mu) = 0.$$

This result provides a powerful tool for analyzing particle motion in curved spacetimes. Each Killing vector corresponds to a continuous symmetry of the metric and gives rise to a conserved physical quantity. For example, time translation symmetry leads to energy conservation, while spatial symmetries lead to conservation of linear or angular momentum.
Therefore, Killing vectors serve as a fundamental bridge between the geometric structure of spacetime and the physical laws governing motion, making them essential in the study of gravitational systems such as black holes and cosmological models [5].

1.2.4 Geodesics

In flat space, the straight line connecting two points has two essential properties. First, it represents the straightest paths, meaning that the tangent vectors at different points on this line remain parallel to each other. Secondly, it represents the shortest path between the two points, and this property is related to the concept of distance defined by the metric $g_{\mu\nu}$. However, in general curved spaces, these two properties do not necessarily coincide. The path that satisfies the property of straightness is generalized to become what is known as the autoparallel curve, where the tangent vectors are transported along it in a parallel manner. In contrast, the concept of the shortest path between two points leads to the definition of the geodesic [16].

1. Derivation of the geodesic equation
   The geodesic is defined as a curve whose tangent vector is parallel transported along itself. If U is the tangent vector [16], this condition is expressed as:

$$\nabla_U U = 0. \tag{1.20}$$

In a local coordinate system (inertial system), these lines are straight. In component form, the geodesic equation:

$$U^\beta \nabla_\beta U^\alpha = U^\beta U^\alpha{}_{;\beta} = U^\beta U^\alpha{}_{,\beta} + \Gamma^\alpha_{\mu\beta} U^\mu U^\beta = 0, \tag{1.21}$$

where $\Gamma^\alpha_{\mu\beta}$ the Christoffel symbols.
If we define λ as the curve parameter, then

$$U^\alpha = \frac{dx^\alpha}{d\lambda}, \quad U^\beta \frac{\partial}{\partial x^\beta} = \frac{d}{d\lambda}. \tag{1.22}$$

Thus, the geodesic equation is written as follows:

$$\frac{d^2 x^\alpha}{d\lambda^2} + \Gamma^\alpha_{\mu\beta} \frac{dx^\mu}{d\lambda} \frac{dx^\beta}{d\lambda} = 0. \tag{1.23}$$

This is a second-order nonlinear differential equation for $x^\alpha(\lambda)$ Given initial conditions at λ_0:

$$x^\alpha(\lambda_0) = x^\alpha_0, \quad U^\alpha_0 = \left.\frac{dx^\alpha}{d\lambda}\right|_{\lambda_0}, \tag{1.24}$$

the solution is unique, defining a single geodesic passing through the point x^α_0 with tangent U^α_0.

Affine Parameterization

If we change the parameter linearly

$$\phi = a\lambda + b, \tag{1.25}$$

where a and b are constants, then ϕ is also an affine parameter in which the geodesic equation retains the same form:

$$\frac{d^2 x^\alpha}{d\phi^2} + \Gamma^\alpha_{\mu\beta} \frac{dx^\mu}{d\phi} \frac{dx^\beta}{d\phi} = 0. \tag{1.26}$$

Only linear transformations of the parameter preserve the geodesic equation. A curve parametrized by a non-affine parameter is not strictly a geodesic, even if it traces the same path.

2. Physical interpretation (free particle motion)
In the context of general relativity, the geodesic is the trajectory a free particle follows in curved spacetime when no external forces are acting on it. In other words, a free particle is one that feels nothing but the force of gravity itself—which is encoded in the geometry of spacetime.
If U is the tangent vector of the particle on its curve, then free motion is expressed by the parallel transport equation(1.20). It means that the covariant acceleration of the particle is zero, which implies that the tangent vector does not change along its path.
can choose the particle's proper time τ as the natural parameter of the geodesic, in which case the tangent vector becomes the four-velocity vector [5].

$$U^\mu = \frac{dx^\mu}{d\tau}. \tag{1.27}$$

For a particle with mass m, motion is also expressed by the four-momentum p, so the free particle equation becomes:

$$p^\nu \nabla_\nu p^\mu = 0. \tag{1.28}$$

This means that the free particle moves along the momentum direction without deviation.
Note on energy: A observer with a four-velocity vector U can measure the energy of a free particle as follows:

$$E = -p_\mu U^\mu.$$

And this formula is valid whether the particle is temporal or light.

1.2.5 Results and Tests of General Relativity

The Effect of Mass on Time (Gravitational Time Dilation)

Gravitational time dilation is a fundamental prediction of general relativity [17], stating that time runs more slowly in stronger gravitational fields. Consider a static, spherically symmetric mass M described by the Schwarzschild metric:

$$ds^2 = -\left(1 - \frac{2GM}{c^2 r}\right) c^2 dt^2 + \left(1 - \frac{2GM}{c^2 r}\right)^{-1} dr^2 + r^2 d\Omega^2,$$

where $d\Omega^2 = d\theta^2 + \sin^2\theta\, d\phi^2$.

For a stationary observer at radius r, the proper time interval $d\tau$ is related to the coordinate time dt by:

$$d\tau = \sqrt{1 - \frac{2GM}{c^2 r}}\, dt.$$

Interpretation: This means that a clock closer to a massive object (smaller r) ticks more slowly than a clock far away from the mass ($r \to \infty$), demonstrating the warping of spacetime by mass.

Example: For Earth, the gravitational time dilation at the surface compared to a distant observer is approximately:

$$\frac{d\tau}{dt} \approx 1 - \frac{GM_\oplus}{c^2 R_\oplus} \approx 1 - 7 \times 10^{-10}.$$

Although small, this effect is measurable and must be corrected in GPS satellite systems.

Light bending

In general relativity, light does not travel in a straight line in the Euclidean sense if it passes near a massive body. Because mass causes the curvature of spacetime, light always travels along a geodesic in spacetime [19].

- The greater the mass, the greater the bending of light.
- This effect is an experimental confirmation of general relativity, and its first observation was during the solar eclipse of 1919.

If a light ray passes near a massive spherical body like the Sun, the deflection angle is approximately

$$\Delta\phi \approx \frac{4GM}{c^2 b},$$

where M the mass of the body (e.g., the Sun), b closest approach distance of the light to the center of the body (impact parameter), G Gravitational constant, c Speed of light.
Light follows a shorter path in curved spacetime, known as a geodesic[5]. It can be imagined as if space is "curved" around the sun, and light follows this curvature.

Gravitational waves

Gravitational waves are ripples in spacetime that propagate at the speed of light. They are generated by accelerating massive, non-symmetric objects, such as merging black holes or neutron stars [17].

In the weak-field approximation, the spacetime metric can be written as:

$$g_{\mu\nu} = \eta_{\mu\nu} + h_{\mu\nu}, \quad |h_{\mu\nu}| \ll 1,$$

where $\eta_{\mu\nu}$ the flat Minkowski metric, $h_{\mu\nu}$ represents a small perturbation.

The perturbations satisfy the linearized wave equation:

$$\Box h_{\mu\nu} = 0, \quad \Box = -\frac{1}{c^2}\frac{\partial^2}{\partial t^2} + \nabla^2.$$

Physical Interpretation Gravitational waves stretch and squeeze spacetime in orthogonal directions (‘"plus" and ‘ "cross" polarizations). They were first directly detected by LIGO in 2015 from the merger of two black holes.

Chapter 2

Black Holes and Dark Matter

2.1 Black Holes

2.1.1 General definition

Black holes are solutions of the field equations of General Relativity that describe regions of spacetime where the gravitational field is strong enough to prevent any form of matter or radiation from escaping. They arise when a sufficient amount of mass is concentrated within a small region, producing a significant curvature of spacetime. In this context, the motion of particles and light follows geodesics determined by the spacetime geometry rather than by a classical force.

As the curvature increases, a surface called the Event Horizon appears. This surface separates the region that can communicate with distant observers from the region that cannot. Any signal generated inside this boundary cannot reach an external observer.

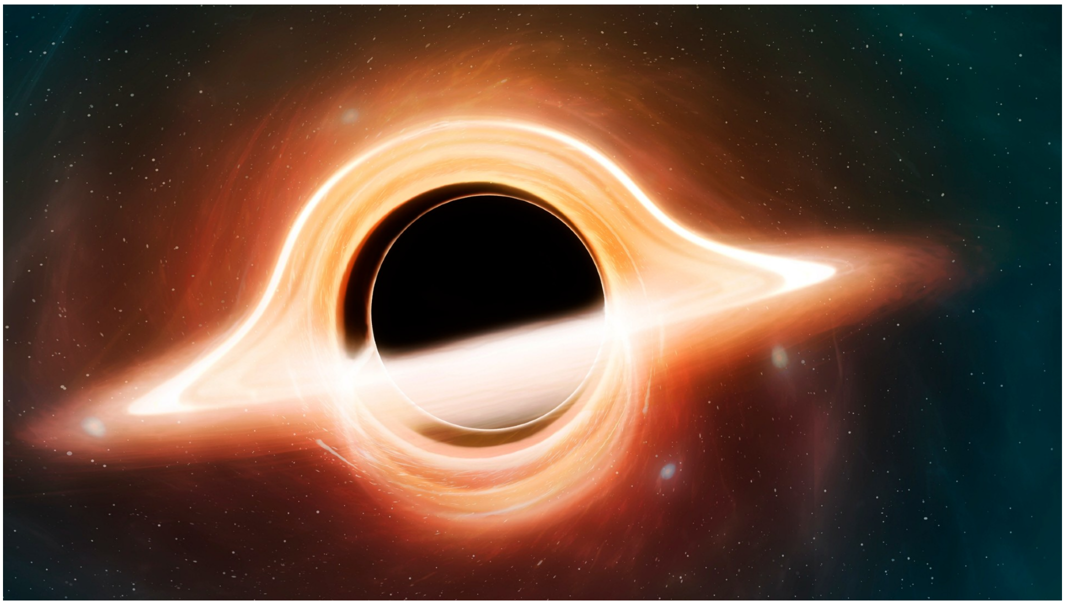

Fig. 2.1 – black hole

Black holes therefore represent exact solutions of the gravitational field equations in which spacetime curvature becomes dominant. Their properties are determined by the geometric structure of spacetime, making them fundamental objects in the study of relativistic gravity rather than merely astrophysical systems. [5].

2.1.2 Properties of Black Holes

Event Horizon

The event horizon is the boundary that separates the inside of a black hole from the rest of the universe. Any particle or light that crosses this boundary cannot escape back out [5], making it the final point of no return. The horizons are the roots of the g^{rr} component of the inverse metric.

$$g^{rr} = 0 \implies r_{\text{Horizon}}. \tag{2.1}$$

Singularity

The singularity of a black hole is a central point where classical general relativity predicts that physical quantities such as density and spacetime curvature become infinite. At this point, the known laws of physics break down [5], and the description of spacetime itself ceases to be meaningful. Mathematically, the singularity is characterized by the divergence of curvature invariants such as the Kretschmann scalar, which for a spherically symmetric black hole is given by:

$$K = R_{\alpha\beta\gamma\delta}R^{\alpha\beta\gamma\delta} = \infty \implies r_{Singularity}, \tag{2.2}$$

where $R_{\alpha\beta\gamma\delta}$ is the Riemann curvature tensor.

This illustrates that the singularity represents a breakdown of the classical spacetime description, requiring a theory of quantum gravity to fully understand the physics at the black hole's core.

Accretion Disk

An accretion disk is a rotating structure of matter formed around a black hole, where gas and dust lose angular momentum and gradually spiral inward under the influence of gravity. In the vicinity of a black hole, the strong spacetime curvature predicted by General Relativity governs the motion of the disk material, forcing it to follow nearly circular geodesic orbits before ultimately plunging toward the central object.

The disk is characterized by differential rotation, where inner regions rotate faster than outer ones, leading to viscous interactions that convert gravitational potential energy into thermal energy. As a result, the accreting matter is heated to very high temperatures and emits electromagnetic radiation across a broad spectrum, often peaking in the X-ray band. This radiation constitutes one of the primary observational signatures of black holes [5].

A key feature of accretion disks is the presence of an inner boundary, commonly associated with the innermost stable circular orbit (ISCO), inside which stable orbits are no longer possible. Beyond this radius, matter rapidly falls toward the black hole, crossing the event horizon. The physical properties of the disk, including its luminosity and spectral distribution, depend strongly on the black hole parameters such as mass and angular momentum and rotation, making accretion disks essential tools for probing the nature of compact objects and testing relativistic gravitational models.

2.1.3 Types of black holes

No-hair theorem

The no-hair theorem states that stationary black holes in general relativity are completely characterized by a limited set of global parameters [7], namely the mass M, electric charge Q, and angular momentum J and thus, the main types of black holes are as follows:

- the Schwarzschild black hole with $M \neq 0$, $J = 0$, $Q = 0$.
- the Kerr black hole with $M \neq 0$, $J \neq 0$, $Q = 0$.
- the Reissner-Nordström black hole with $M \neq 0$, $J = 0$, $Q \neq 0$.
- the Kerr-Newman black hole with $M \neq 0$, $J \neq 0$, $Q \neq 0$.

2.1.4 Schwarzschild Black Hole

The Schwarzschild solution, discovered by Karl Schwarzschild in 1916, is considered one of the most important exact solutions to Einstein's equations, as it describes the external gravitational field of a stationary spherical body like the sun. Due to its perfect spherical symmetry, the spacetime geometry depends only on the radial coordinate. These features make the Schwarzschild black hole a fundamental reference model for the study of black holes, providing a basis for more general solutions such as the charged RN and the rotating Kerr black holes [7].

The Metric

The Schwarzschild metric is the exact solution of Einstein's field equations in vacuum, describing the spacetime geometry outside a static, spherically symmetric, and uncharged mass.

$$ds^2 = -\left(1 - \frac{2GM}{c^2 r}\right) c^2 dt^2 + \left(1 - \frac{2GM}{c^2 r}\right)^{-1} dr^2 + r^2 (d\theta^2 + \sin^2\theta \, d\phi^2), \tag{2.3}$$

where G Newton's gravitational constant, M Mass of the central object.

Event Horizon

To find the event horizon, we use the equation (2.1):

$$g^{rr} = 1 - \frac{2GM}{c^2 r} = 0, \tag{2.4}$$

$$r_H = \frac{2GM}{c^2}. \tag{2.5}$$

This radius corresponds to the event horizon of a Schwarzschild black hole.

For $r > r_s$, the metric describes the exterior gravitational field. At $r = r_s$, the metric exhibits a coordinate singularity, while at $r = 0$, a true physical singularity is present.

This behavior indicates a coordinate singularity rather than a physical one. The event horizon represents a causal boundary beyond which no signal or particle can escape to an external observer.

Singularity Using the equation (2.2) we get:

$$K = R_{\mu\nu\rho\sigma}R^{\mu\nu\rho\sigma} = \frac{48G^2M^2}{r^6}, \tag{2.6}$$

When $r \to 0$, we have $K \to \infty$, meaning that we have a true physical singularity at

$$r_{Sing} = 0. \tag{2.7}$$

Therefore, $r = 0$ is not a coordinate singularity but an intrinsic feature of spacetime where physical quantities such as density and tidal forces become infinite.

2.1.5 Reissner–Nordström Black Hole

The RN black hole exhibits several important physical properties. It is a static and spherically symmetric spacetime characterized by the presence of an electric charge in addition to its mass. In the case of $Q = 0$, it becomes a Schwarzschild solution. The spacetime has a more complex causal structure than the uncharged case, including the presence of two horizons [5].

The metric

In Schwarzschild coordinates (t, r, θ, ϕ), the RN metric is given by

$$ds^2 = -f(r)\,dt^2 + \frac{1}{f(r)}dr^2 + r^2d\theta^2 + r^2\sin^2\theta\,d\phi^2. \tag{2.8}$$

Where the metric function is defined as follows:

$$f(r) = 1 - \frac{2M}{r} + \frac{Q^2}{r^2}. \tag{2.9}$$

Here M represents the mass of the black hole and Q its electric charge.

Event Horizon

The horizons of the RN black hole are determined by the roots of $f(r) = 0$ in equation (2.9):

$$r_H = r_\pm = M \pm \sqrt{M^2 - Q^2}. \tag{2.10}$$

According to the values of M and Q, we have three distinct cases:

First case:	$M^2 > Q^2 \implies$	two horizons,
Second case:	$M^2 = Q^2 \implies$	one horizons,
Third case:	$M^2 < Q^2 \implies$	no horizons.

• When $M^2 > Q^2$, Unlike the Schwarzschild case which has only one horizon, the presence of charge Q modifies the spacetime structure, resulting in an inner and an outer horizon, r_+ and r_- respectively.

• When $M^2 = Q^2$, the black hole is called extremal, which is characterized by only one horizon r_H concealing the singularity $r_{sing} = 0$.

• When $M^2 < Q^2$, r_H is not real and there is no horizon concealing the singularity $r_{sing} = 0$ from the rest of spacetime.

Singularity

The curvature of RN spacetime can be characterized by the Kretschmann scalar, given by:

$$K = R_{\mu\nu\rho\sigma}R^{\mu\nu\rho\sigma} = \frac{48M^2}{r^6} - \frac{96MQ^2}{r^7} + \frac{56Q^4}{r^8}. \tag{2.11}$$

The spacetime of RN contains a point of curvature singularity located at:

$$K \to \infty \quad \text{as} \quad r_{Sing} = 0 \tag{2.12}$$

In the RN solution, the singularity $r = 0$ is hidden behind the event horizons when $M^2 \geq Q^2$. Therefore, it is not visible to an external observer. However, if $Q^2 > M^2$, no horizons exist and the singularity becomes naked, meaning it is visible to distant observers.

2.1.6 Kerr Black Hole

The Kerr black hole is an exact, stationary, and axisymmetric solution of the Einstein field equations that describes the spacetime geometry around a rotating, uncharged mass. Discovered in 1963 by Roy Kerr, characterized by a non-zero angular momentum. In the limit where the rotation parameter $a = 0$, the Kerr metric reduces to the Schwarzschild solution [6].

The metric

In Boyer-Lindquist coordinates (t, r, θ, ϕ), the Kerr metric takes the form [7]:

$$ds = -\left(1 - \frac{2Mr}{\Sigma}\right) dt - \frac{4Mar\sin^2\theta}{\Sigma} dt\, d\phi + \frac{\Sigma}{\Delta} dr + \Sigma\, d\theta^2 + \left(r + a^2 + \frac{2Ma^2 r\sin^2\theta}{\Sigma}\right) \sin^2\theta\, d\phi^2, \tag{2.13}$$

where the metric functions are defined as

$$\Sigma = r^2 + a^2\cos^2\theta\,, \quad \Delta = r^2 - 2Mr + a^2. \tag{2.14}$$

Here M represents the mass of the black hole and $a = \frac{J}{M}$ is the specific angular momentum.

Event Horizons

The horizons of the Kerr black hole are determined by the roots of $\Delta = 0$ in equation (2.14)

$$r_H = r_\pm = M \pm \sqrt{M^2 - a^2}. \tag{2.15}$$

The outer horizon r_+ corresponds to the event horizon, while the inner horizon r_- is known as the Cauchy horizon.

Singularity

The curvature of spacetime in the Kerr black hole can be characterized by the Kretschmann scalar, which is defined as follows:

$$K = R_{\mu\nu\rho\sigma}R^{\mu\nu\rho\sigma} = \frac{48M^2\left(r^6 - 15a^2r^4\cos^2\theta + 15a^4r^2\cos^4\theta - a^6\cos^6\theta\right)}{\left(r^2 + a^2\cos^2\theta\right)^6}. \tag{2.16}$$

Unlike the Schwarzschild black hole, which has a point-like singularity, the Kerr black hole possesses a ring-shaped singularity. This singularity occurs at:

$$K \to \infty \quad \Longrightarrow \quad (r_{Sing} = 0, \quad \theta_{Sing} = \frac{\pi}{2}). \tag{2.17}$$

This corresponds to a ring singularity.

2.1.7 Kerr–Newman Black Hole

The Kerr-Newman black hole is a stationary, axisymmetric solution characterized by mass M, angular momentum J, and electric charge Q, with specific angular momentum $a = \frac{J}{M}$.

The metric

In Boyer-Lindquist coordinates (t, r, θ, ϕ), the metric is given by

$$\begin{aligned} ds^2 = &-\left(1 - \frac{2Mr - Q^2}{\Sigma}\right) dt^2 - \frac{2a(2Mr - Q^2)\sin^2\theta}{\Sigma}\, dt\, d\phi + \frac{\Sigma}{\Delta}\, dr^2 + \Sigma\, d\theta^2 \\ &+ \left(r^2 + a^2 + \frac{(2Mr - Q^2)a^2 \sin^2\theta}{\Sigma}\right) \sin^2\theta\, d\phi^2, \end{aligned} \tag{2.18}$$

where

$$\Sigma = r^2 + a^2 \cos^2\theta, \tag{2.19}$$

$$\Delta = r^2 - 2Mr + a^2 + Q^2. \tag{2.20}$$

Horizons

The horizons are obtained from the equation $\Delta = 0$:

$$r_H = r_\pm = M \pm \sqrt{M^2 - a^2 - Q^2}. \tag{2.21}$$

Thus, the condition for the existence of a black hole is $M^2 \geq a^2 + Q^2$.

Singularity

The Kretschmann scalar is given by

$$K = R_{\mu\nu\rho\sigma} R^{\mu\nu\rho\sigma} = \frac{8\left[6M^2(r^2 - a^2\cos^2\theta)^2 - 12MQ^2 r(r^2 - a^2\cos^2\theta) + Q^4(7r^2 - a^2\cos^2\theta)\right]}{(r^2 + a^2\cos^2\theta)^6}. \tag{2.22}$$

Thus, the singularity occurs at:

$$K \to \infty \quad \Longrightarrow \quad (r_{Sing} = 0, \quad \theta_{Sing} = \frac{\pi}{2}). \tag{2.23}$$

This corresponds to a ring singularity, similar to the Kerr black hole, but influenced by the presence of charge [?].

Types of Black Holes according to the mass

1. Stellar black holes
   Stellar black holes are one of the fundamental types of black holes, formed as a result of the gravitational collapse of a massive star at the end of its life cycle. When the star exhausts its nuclear fuel, it loses the internal pressure that was opposing the force of gravity, leading to a catastrophic collapse of its core under the influence of its weight. If the mass of the core remaining after the stellar explosion (usually in the form of a supernova) is greater than a certain limit known as the Tolman-Oppenheimer-Volkoff (TOV limit) [5].

Stellar black holes are characterized by masses that typically range from about 3 to tens of solar masses, making them much smaller than the supermassive black holes found at the centers of galaxies. These black holes are surrounded by an event horizon, which is the boundary surface that defines the point beyond which escape becomes impossible, like a Schwarzschild black hole and RN black hole.

2. Supermassive black holes
Supermassive black holes exist at the centers of most galaxies, including the Milky Way like Sagittarius A* . These black holes are characterized by enormous masses ranging from millions to billions of solar masses, extending their gravitational influence over a vast area within the galaxy. As for their formation, it is believed that these black holes arise through several integrated mechanisms, including the gradual growth of a primordial black hole through the accumulation of surrounding material and its merger with other black holes, in addition to the possibility that some formed directly in the early universe due to the direct collapse of massive gas clouds. Galactic mergers also significantly increase its mass through the merging of central black holes. [17].

3. Intermediate-mass black holes
Intermediate-mass black holes (IMBHs) like HLX-1 represent a gravitational system in the intermediate mass range, typically satisfying the range $0^2 \lesssim M/M_\odot \lesssim 10^5$, making them a dynamic bridge between stellar-mass black holes and supermassive black holes. In the framework of general relativity, these objects are described by solutions to the Einstein field equations, where the curvatures of spacetime determine the structure of the event horizon and the Schwarzschild radius, which is linearly proportional to the mass. Observationally, it is difficult to detect intermediate-mass black holes, as they typically do not produce strong electromagnetic signatures like active galactic nuclei, and their gravitational influence is weaker compared to supermassive black holes.

2.2 Derivation of Spherically Symmetric Metrics

2.2.1 Derivation Schwarzschild metric

Metric Ansatz

Second assuming a static and spherically symmetric spacetime, the most general form of the metric is:

$$ds^2 = -e^{2\Phi(r)}dt^2 + e^{-2\Lambda(r)}dr^2 + r^2 d\theta^2 + r^2 \sin^2\theta \, d\phi^2, \tag{2.24}$$

where $\Phi(r)$ and $\Lambda(r)$ are unknown functions to be determined [5].

Christoffel Symbols

The non-vanishing Christoffel symbols are:

$$\begin{aligned}
&\Gamma^t_{tr} = \Phi'(r), \quad \Gamma^r_{tt} = e^{2(\Phi-\Lambda)}\Phi'(r), \quad \Gamma^r_{rr} = \Lambda'(r), \\
&\Gamma^r_{\theta\theta} = -re^{-2\Lambda}, \quad \Gamma^r_{\phi\phi} = -r\sin^2\theta \, e^{-2\Lambda}, \quad \Gamma^\theta_{r\theta} = \Gamma^\phi_{r\phi} = \frac{1}{r}.
\end{aligned}$$

Ricci Tensor Components

After computing the Ricci tensor, we obtain:

$$\begin{aligned}
R_{tt} &= e^{2(\Phi-\Lambda)}\left[\Phi'' + (\Phi')^2 - \Phi'\Lambda' + \frac{2}{r}\Phi'\right],\\
R_{rr} &= -\Phi'' - (\Phi')^2 + \Phi'\Lambda' + \frac{2}{r}\Lambda',\\
R_{\theta\theta} &= 1 - e^{-2\Lambda}\left(1 - r\Lambda' + r\Phi'\right).
\end{aligned}$$

Ricci scale

In the Schwarzschild metric, the Ricci scalar is zero because the spacetime is a vacuum $T_{\mu\nu} = 0$; therefore, from the Einstein field equations, it follows that (R = 0).

$$R_{\mu\nu} = 0,$$

$$R = g^{\mu\nu}R_{\mu\nu} = 0.$$

Einstein Equations

we have $T_{\mu\nu} = 0$ the Einstein equation.

$$R_{\mu\nu} - \frac{1}{2}R\,g_{\mu\nu} = \frac{8\pi G}{c^4}T_{\mu\nu} \tag{2.25}$$

$$R_{\mu\nu} - \frac{1}{2}R\,g_{\mu\nu} = 0 \tag{2.26}$$

By substituting R, g into Einstein's equations, we get

$$R_{tt} - \frac{1}{2}g_{tt}R = 0, \tag{2.27}$$
$$R_{rr} - \frac{1}{2}g_{rr}R = 0, \tag{2.28}$$
$$R_{\theta\theta} - \frac{1}{2}g_{\theta\theta}R = 0, \tag{2.29}$$
$$R_{\phi\phi} - \frac{1}{2}g_{\phi\phi}R = 0. \tag{2.30}$$

We divide the equations (2.27) and (2.28) by $g_{\mu\nu}$, we get:

$$\begin{aligned}
\frac{R_{tt} - \frac{1}{2}g_{tt}R}{g_{tt}} &= -\frac{R_{rr} - \frac{1}{2}g_{rr}R}{g_{rr}}\\
\frac{R_{tt}}{g_{tt}} - \frac{1}{2}R &= -\frac{R_{rr}}{g_{rr}} - \frac{1}{2}R\\
\frac{R_{tt}}{g_{tt}} &= -\frac{R_{rr}}{g_{rr}}\\
R_{tt}e^{-2\Phi} &= -R_{rr}e^{-2\Lambda}
\end{aligned}$$

We equalize both equations:

$$\begin{aligned}
e^{-2\Lambda}\Big[\Phi'' + \Phi'^2 - \Phi'\Lambda' + \frac{2}{r}\Phi'\Big] &= e^{-2\Lambda}\Big[-\Phi'' - \Phi'^2 + \Phi'\Lambda' + \frac{2}{r}\Lambda'\Big] \\
\Phi'' + \Phi'^2 - \Phi'\Lambda' + \frac{2}{r}\Phi' &= -(-\Phi'' - \Phi'^2 + \Phi'\Lambda' + \frac{2}{r}\Lambda') \\
\frac{1}{r}(\Phi' + \Lambda') &= 0 \\
\Phi' + \Lambda' &= 0 \\
\Phi &= -\Lambda + C \qquad (2.31)
\end{aligned}$$

Thus C_1 and C_2 are integration constants that can be identified Using the Newtonian limit $e^{-2\Lambda} \approx 1 - \frac{2M}{r}$

$$f(r) = e^{-2\Lambda} \to 1 - \frac{2M}{r}, \qquad (2.32)$$

$$\implies C_1 = 1\ , \quad C_2 = -2M, \qquad (2.33)$$

Final Metric:

Substituting into the metric:

$$ds^2 = -\left(1 - \frac{2GM}{c^2 r}\right)c^2 dt^2 + \left(1 - \frac{2GM}{c^2 r}\right)^{-1} dr^2 + r^2(d\theta^2 + \sin^2\theta\, d\phi^2), \qquad (2.34)$$

where G Newton's gravitational constant, M mass of the central object, c speed of light, r radial coordinate, (θ, ϕ) angular coordinate, and t time coordinate measured by a distant observer.

2.2.2 Derivation of the Reissner-Nordström metric

In this section, we will derive the RN solution by solving the Einstein field equations in the presence of an electromagnetic field.
The first step is spherical symmetry ansatz. We assume a static and spherically symmetric spacetime. The most general form of the metric can then be written as:

$$ds^2 = -e^{2\Phi(r)}dt^2 + e^{2\Lambda(r)}dr^2 + r^2 d\Omega^2, \qquad (2.35)$$

where $d\Omega^2 = d\theta^2 + \sin^2\theta\, d\phi^2$. Then components of the metric $g_{\mu\nu}$ are given by:

$$g_{tt} = -e^{2\Phi(r)}, \quad g_{rr} = e^{2\Lambda(r)}, \quad g_{\theta\theta} = r^2, \quad g_{\phi\phi} = r^2\sin^2\theta. \qquad (2.36)$$

The components of the inverse metric $g^{\mu\nu}$ are given by:

$$g^{tt} = -e^{-2\Phi(r)}, \quad g^{rr} = e^{-2\Lambda(r)}, \quad g^{\theta\theta} = \frac{1}{r^2}, \quad g^{\phi\phi} = \frac{1}{r^2\sin^2\theta}. \qquad (2.37)$$

The second step is to calculate the Christoffel symbols. The christoffel symbols are given by this equation

$$\Gamma^\alpha_{\mu\nu} = \frac{1}{2}g^{\alpha\beta}\left(\partial_\mu g_{\nu\beta} + \partial_\nu g_{\mu\beta} - \partial_\beta g_{\mu\nu}\right). \qquad (2.38)$$

By substituting from (3.5) in (2.38) we obtain

$$\begin{aligned}
&\Gamma^t_{tr} = \Phi'(r), \quad \Gamma^r_{tt} = e^{2(\Phi-\Lambda)}\Phi'(r), \quad \Gamma^r_{rr} = \Lambda'(r), \\
&\Gamma^r_{\theta\theta} = -re^{-2\Lambda}, \quad \Gamma^r_{\phi\phi} = -r\sin^2\theta\, e^{-2\Lambda}, \quad \Gamma^\theta_{r\theta} = \Gamma^\phi_{r\phi} = \frac{1}{r}.
\end{aligned} \qquad (2.39)$$

The third step is to calculate the Ricci tensor. The Ricci tensor is obtained by contracting the Riemann tensor:

$$R_{\mu\nu} = R^{\alpha}{}_{\mu\alpha\nu}, \tag{2.40}$$

$$R_{\mu\nu} = \partial_\alpha \Gamma^\alpha_{\mu\nu} - \partial_\nu \Gamma^\alpha_{\mu\alpha} + \Gamma^\alpha_{\beta\alpha}\Gamma^\beta_{\mu\nu} - \Gamma^\alpha_{\beta\nu}\Gamma^\beta_{\mu\alpha}. \tag{2.41}$$

From the definition of the Ricci tensor (3.7), the ttcomponent is found to be:

$$\begin{aligned}
R_{tt} &= \partial_\alpha \Gamma^\alpha_{tt} - \partial_t \Gamma^\alpha_{t\alpha} + \Gamma^\alpha_{\beta\alpha}\Gamma^\beta_{tt} - \Gamma^\alpha_{\beta t}\Gamma^\beta_{t\alpha},\\
R_{tt} &= \partial_r \Gamma^r_{tt} + \Gamma^r_{rr}\Gamma^r_{tt} + \Gamma^\theta_{\theta r}\Gamma^r_{tt} + \Gamma^\phi_{\phi r}\Gamma^r_{tt} - (\Gamma^r_{tt})^2,\\
R_{tt} &= \partial_r \Gamma^r_{tt} + (\Gamma^r_{rr} + \Gamma^\theta_{\theta r} + \Gamma^\phi_{\phi r})\Gamma^r_{tt} - (\Gamma^r_{tt})^2,\\
R_{tt} &= \partial_r \left(e^{2(\Phi-\Lambda)}\Phi'\right) + \left(\Lambda' + \frac{2}{r}\right) e^{2(\Phi-\Lambda)}\Phi' - \left(e^{2(\Phi-\Lambda)}\Phi'\right)^2,\\
R_{tt} &= e^{2(\Phi-\Lambda)}\left[\Phi'' + 2\Phi'^2 - 2\Phi'\Lambda'\right] \quad + \left(\Lambda' + \frac{2}{r}\right) e^{2(\Phi-\Lambda)}\Phi' - e^{4(\Phi-\Lambda)}\Phi'^2,\\
R_{tt} &= e^{2(\Phi-\Lambda)}\left[\Phi'' + 2\Phi'^2 - 2\Phi'\Lambda' + \left(\Lambda' + \frac{2}{r}\right)\Phi' - e^{2(\Phi-\Lambda)}\Phi'^2\right],\\
R_{tt} &= e^{2(\Phi-\Lambda)}\left[\Phi'' + \Phi'^2 - \Phi'\Lambda' + \frac{2}{r}\Phi'\right].
\end{aligned} \tag{2.42}$$

Using equation (3.7), the rrcomponent is found to be:

$$\begin{aligned}
R_{rr} &= \partial_\alpha \Gamma^\alpha_{rr} - \partial_r \Gamma^\alpha_{r\alpha} + \Gamma^\alpha_{\beta\alpha}\Gamma^\beta_{rr} - \Gamma^\alpha_{\beta r}\Gamma^\beta_{r\alpha},\\
R_{rr} &= \partial_r \Gamma^r_{rr} - \partial_r(\Gamma^t_{rt} + \Gamma^r_{rr} + \Gamma^\theta_{r\theta} + \Gamma^\phi_{r\phi}) \quad + (\Gamma^r_{rr} + \Gamma^\theta_{\theta r} + \Gamma^\phi_{\phi r})\Gamma^r_{rr} - (\Gamma^t_{rr})^2,\\
R_{rr} &= \Lambda'' - (\Phi'' + \Lambda'' - \frac{2}{r^2}) + \left(\Lambda' + \frac{2}{r}\right)\Lambda' - (\Phi')^2,\\
R_{rr} &= -\Phi'' - (\Phi')^2 + \Lambda'\Phi' + \frac{2}{r}\Lambda',\\
R_{rr} &= -\Phi'' - \Phi'^2 + \Phi'\Lambda' + \frac{2}{r}\Lambda'.
\end{aligned} \tag{2.43}$$

From equation (3.7), the $\theta\theta$component is found to be:

$$\begin{aligned}
R_{\theta\theta} &= \partial_\alpha \Gamma^\alpha_{\theta\theta} - \partial_\theta \Gamma^\alpha_{\theta\alpha}\Gamma^\alpha_{\beta\theta}\Gamma^\beta_{\theta\alpha},\\
R_{\theta\theta} &= \partial_r \Gamma^r_{\theta\theta} + (\Gamma^r_{rr} + \Gamma^\theta_{\theta r} + \Gamma^\phi_{\phi r})\Gamma^r_{\theta\theta} - (\Gamma^\phi_{\theta\phi})^2,\\
R_{\theta\theta} &= \left[-e^{-2\Lambda} + 2r\Lambda' e^{-2\Lambda}\right] + \left(\Lambda' + \frac{2}{r}\right)(-re^{-2\Lambda}) - \cot^2\theta,\\
R_{\theta\theta} &= 1 - e^{-2\Lambda}(1 - r\Lambda' + r\Phi').
\end{aligned} \tag{2.44}$$

Using equation (3.7), the $\phi\phi$component is found to be:

$$\begin{aligned}
R_{\phi\phi} &= \partial_\alpha \Gamma^\alpha_{\phi\phi} - \partial_\phi \Gamma^\alpha_{\phi\alpha} + \Gamma^\alpha_{\beta\alpha}\Gamma^\beta_{\phi\phi} - \Gamma^\alpha_{\beta\phi}\Gamma^\beta_{\phi\alpha},\\
R_{\phi\phi} &= \partial_r \Gamma^r_{\phi\phi} + (\Gamma^r_{rr} + \Gamma^\theta_{\theta r} + \Gamma^\phi_{\phi r})\Gamma^r_{\phi\phi} - (\Gamma^\theta_{\phi\theta})^2 - (\Gamma^\phi_{\phi\phi})^2,\\
R_{\phi\phi} &= \left[-e^{-2\Lambda} + 2r\Lambda' e^{-2\Lambda}\right]\sin^2\theta + \left(\Lambda' + \frac{2}{r}\right)(-re^{-2\Lambda}\sin^2\theta) + \sin^2\theta,\\
R_{\phi\phi} &= \sin^2\theta\, r^2\left[1 - e^{-2\Lambda}(1 - r\Lambda' + r\Phi')\right],
\end{aligned}$$

$$R_{\phi\phi} = \sin^2\theta\,\left[1 - e^{-2\Lambda}(1 - r\Lambda' + r\Phi')\right], \tag{2.45}$$

$$R_{\phi\phi} = \sin^2\theta\, R_{\theta\theta}. \tag{2.46}$$

The fourth step is to calculate Ricci scalar. The Ricci scalar is given by this definition:

$$\begin{aligned}
R &= g^{\mu\nu}R_{\mu\nu},\\
R &= g^{tt}R_{tt} + g^{rr}R_{rr} + g^{\theta\theta}R_{\theta\theta} + g^{\phi\phi}R_{\phi\phi},\\
R &= -e^{-2\Phi}R_{tt} + e^{-2\Lambda}R_{rr} + \frac{1}{r^2}R_{\theta\theta} + \frac{1}{r^2\sin^2\theta}(\sin^2\theta R_{\theta\theta}),\\
R &= -e^{-2\Phi}\left[e^{2(\Phi-\Lambda)}(\Phi'' + \Phi'^2 - \Phi'\Lambda' + \frac{2}{r}\Phi')\right] + e^{-2\Lambda}\left[-\Phi'' - \Phi'^2 + \Phi'\Lambda' + \frac{2}{r}\Lambda'\right]\\
&\quad + \frac{2}{r^2}\left[1 - e^{-2\Lambda}(1 - r\Lambda' + r\Phi')\right],\\
R &= e^{-2\Lambda}\left[-2\Phi'' - 2\Phi'^2 + 2\Phi'\Lambda' + \frac{2}{r}(\Lambda' - \Phi')\right] + \frac{2}{r^2}(1 - e^{-2\Lambda}) + \frac{2}{r}e^{-2\Lambda}(\Lambda' - \Phi'),\\
R &= \frac{2}{r^2}(1 - e^{-2\Lambda}) + e^{-2\Lambda}\left[-2\Phi'' - 2\Phi'^2 + 2\Phi'\Lambda' + \frac{4}{r}(\Lambda' - \Phi')\right]. \qquad (2.47)
\end{aligned}$$

The fifth step is to calculate the energy-momentum tensor. In this case, the energy-momentum tensor is non-zero and corresponds to the electromagnetic field:

$$T_{\mu\nu} = \frac{1}{4\pi}\left(F_{\mu\alpha}F_{\nu}{}^{\alpha} - \frac{1}{4}g_{\mu\nu}F_{\alpha\beta}F^{\alpha\beta}\right). \qquad (2.48)$$

For an electric charge:

$$F_{tr} = -F_{rt} = \frac{Q}{r^2} \;\Rightarrow\; F_{\alpha\beta}F^{\alpha\beta} = -\frac{2Q^2}{r^4}.$$

Thus, the energy-momentum tensor of the electromagnetic field is given by:

$$T_{tt} = \frac{Q^2}{8\pi r^4}g_{tt}, \qquad (2.49)$$

$$T_{rr} = -\frac{Q^2}{8\pi r^4}g_{rr}, \qquad (2.50)$$

$$T_{\theta\theta} = \frac{Q^2}{8\pi r^4}g_{\theta\theta}, \qquad (2.51)$$

$$T_{\phi\phi} = \frac{Q^2}{8\pi r^4}\,g_{\phi\phi}. \qquad (2.52)$$

$$\qquad (2.53)$$

The sixth step Einstein Equations

$$R_{\mu\nu} - \frac{1}{2}R\,g_{\mu\nu} = \frac{8\pi G}{c^4}\,T_{\mu\nu},$$

Where $R_{\mu\nu}$ the Ricci tensor and R the Ricci scalar. By substituting R, g and T into Einstein's equations, we get:

$$R_{tt} - \frac{1}{2}g_{tt}R = \frac{Q^2}{r^4}g_{tt}, \qquad (2.54)$$

$$R_{rr} - \frac{1}{2}g_{rr}R = -\frac{Q^2}{r^4}g_{rr}, \qquad (2.55)$$

$$R_{\theta\theta} - \frac{1}{2}g_{\theta\theta}R = \frac{Q^2}{r^4}\,g_{\theta\theta}, \qquad (2.56)$$

$$R_{\phi\phi} - \frac{1}{2}g_{\phi\phi}R = \frac{Q^2}{r^4}\,g_{\phi\phi}. \qquad (2.57)$$

We divide the equations (2.54)and(2.55) by $g_{\mu\nu}$, we get:

$$
\begin{aligned}
\frac{R_{tt} - \frac{1}{2}g_{tt}R}{g_{tt}} &= -\frac{R_{rr} - \frac{1}{2}g_{rr}R}{g_{rr}} \\
\frac{R_{tt}}{g_{tt}} - \frac{1}{2}R &= -\frac{R_{rr}}{g_{rr}} - \frac{1}{2}R \\
\frac{R_{tt}}{g_{tt}} &= -\frac{R_{rr}}{g_{rr}} \\
R_{tt}e^{-2\Phi} &= -R_{rr}e^{-2\Lambda}
\end{aligned}
$$

We equalize both equations:

$$
\begin{aligned}
e^{-2\Lambda}\Big[\Phi'' + \Phi'^2 - \Phi'\Lambda' + \frac{2}{r}\Phi'\Big] &= e^{-2\Lambda}\Big[-\Phi'' - \Phi'^2 + \Phi'\Lambda' + \frac{2}{r}\Lambda'\Big] \\
\Phi'' + \Phi'^2 - \Phi'\Lambda' + \frac{2}{r}\Phi' &= -(-\Phi'' - \Phi'^2 + \Phi'\Lambda' + \frac{2}{r}\Lambda') \\
\frac{1}{r}(\Phi' + \Lambda') &= 0 \\
\Phi' + \Lambda' &= 0 \\
\Phi &= -\Lambda + C
\end{aligned}
\tag{2.58}
$$

The constant C can be removed by a redefinition of the time coordinate $t \to \tilde{t}$, so that the metric coefficient can be rescaled without loss of generality. Consequently, we obtain

$$
\Phi = -\Lambda \tag{2.59}
$$

By substituting this result in (3.10):

$$
\begin{aligned}
R_{\theta\theta} &= 1 - e^{-2\Lambda}(1 - r\Lambda' + r\Phi'), \\
R_{\theta\theta} &= 1 - e^{-2\Lambda}(1 - r\Lambda' - r\Lambda'), \\
R_{\theta\theta} &= 1 - e^{-2\Lambda}(1 - 2r\Lambda'), \\
R_{\theta\theta} &= 1 - e^{-2\Lambda} + 2r\Lambda' e^{-2\Lambda}.
\end{aligned}
$$

By substituting (2.59) in Ricci scalar

$$
\begin{aligned}
R &= \frac{2}{r^2}(1 - e^{-2\Lambda}) + e^{-2\Lambda}\left[-2\Phi'' - 2\Phi'^2 + 2\Phi'\Lambda' + \frac{4}{r}(\Lambda' - \Phi')\right], \\
R &= \frac{2}{r^2}(1 - e^{-2\Lambda}) + e^{-2\Lambda}\left[2\Lambda'' - 2\Lambda'^2 - 2\Lambda'\Lambda' + \frac{4}{r}(\Lambda' + \Lambda')\right], \\
R &= \frac{2}{r^2}(1 - e^{-2\Lambda}) + e^{-2\Lambda}\left[2\Lambda'' - 2\Lambda'^2 - 2\Lambda'^2 + \frac{4}{r}(2\Lambda')\right], \\
R &= \frac{2}{r^2}(1 - e^{-2\Lambda}) + e^{-2\Lambda}\left[2\Lambda'' - 4\Lambda'^2 + \frac{8}{r}(\Lambda')\right].
\end{aligned}
$$

Inserting the previous result, we get:

$$
R_{\theta\theta} - \frac{1}{2}g_{\theta\theta}R = \frac{Q^2}{r^4}\, g_{\theta\theta},
$$

$$R_{\theta\theta} - \frac{1}{2}r^2 R = \frac{Q^2}{r^4}r^2,$$

$$1 - e^{-2\Lambda} + 2r\Lambda' e^{-2\Lambda} - \frac{1}{2}r^2\left[\frac{2}{r^2}(1-e^{-2\Lambda}) + e^{-2\Lambda}\left[2\Lambda'' - 4\Lambda'^2 + \frac{8}{r}(\Lambda')\right]\right] = \frac{Q^2}{r^2},$$

$$2r\Lambda' e^{-2\Lambda} + r^2 e^{-2\Lambda}\left[-\Lambda'' + 2\Lambda'^2 - \frac{4}{r}(\Lambda')\right] = \frac{Q^2}{r^2},$$

$$r^2 e^{-2\Lambda}\left(-\Lambda'' + 2(\Lambda')^2 - \frac{2}{r}\Lambda'\right) = \frac{Q^2}{r^2}, \tag{2.60}$$

On the other hand, we have $(r^2 e^{-2\Lambda})$

$$\frac{d}{dr}\left(re^{-2\Lambda}\right) = e^{-2\Lambda} + r\left(-2\Lambda' e^{-2\Lambda}\right),$$
$$= e^{-2\Lambda}\left(1 - 2r\Lambda'\right).$$

We derive it for the second time.

$$\frac{d^2}{dr^2}\left(re^{-2\Lambda}\right) = \frac{d}{dr}\left[e^{-2\Lambda}\left(1-2r\Lambda'\right)\right],$$
$$= (-2\Lambda' e^{-2\Lambda})(1-2r\Lambda') + e^{-2\Lambda}(-2\Lambda' - 2r\Lambda''),$$
$$= e^{-2\Lambda}\left[-2\Lambda'(1-2r\Lambda') - 2\Lambda' - 2r\Lambda''\right],$$
$$= e^{-2\Lambda}\left[-2\Lambda' + 4r(\Lambda')^2 - 2\Lambda' - 2r\Lambda''\right],$$
$$= e^{-2\Lambda}\left[-4\Lambda' + 4r(\Lambda')^2 - 2r\Lambda''\right],$$

$$\frac{r}{2}\frac{d^2}{dr^2}\left(re^{-2\Lambda}\right) = r^2 e^{-2\Lambda}\left[-\Lambda'' + 2(\Lambda')^2 - \frac{2}{r}\Lambda'\right]. \tag{2.61}$$

We found (3.22)and(3.23) are equal, so we use The simplified form and we integrate the expression

$$\frac{r}{2}\frac{d^2}{dr^2}\left(re^{-2\Lambda}\right) = \frac{Q^2}{r^2},$$

$$\frac{d^2}{dr^2}\left(re^{-2\Lambda}\right) = \int \frac{Q^2}{r^3},$$

$$\frac{d}{dr}\left(re^{-2\Lambda}\right) = \int \frac{Q^2}{r^2} + C_1,$$

$$re^{-2\Lambda} = \frac{Q^2}{r} + C_1 r + C_2,$$

$$e^{-2\Lambda} = C_1 + \frac{C_2}{r} + \frac{Q^2}{r^2}. \tag{2.62}$$

Using the Newtonian limit $e^{-2\Lambda} \to 1 - \frac{2M}{r}$, we get

$$C_1 = 1, C_2 = -2M,$$

$$\Rightarrow\ e^{-2\Lambda} = 1 - \frac{2M}{r} + \frac{Q^2}{r^2}.$$

Thus, the RN metric takes the form:

$$ds^2 = -\left(1 - \frac{2M}{r} + \frac{Q^2}{r^2}\right) dt^2 + \left(1 - \frac{2M}{r} + \frac{Q^2}{r^2}\right)^{-1} dr^2 + r^2 d\Omega^2. \tag{2.63}$$

The Einstein–Maxwell equations reduce, under spherical symmetry and the condition $\Phi = -\Lambda$, to a single differential equation that can be written in a total derivative form. Its integration yields the RN metric, describing a static charged black hole characterized by mass M and electric charge Q.

In the image(2.2), we plotted the function $f(r)$ with respect to r for three values of $\frac{Q}{M} = (0, 1, 0.6)$, we obtain

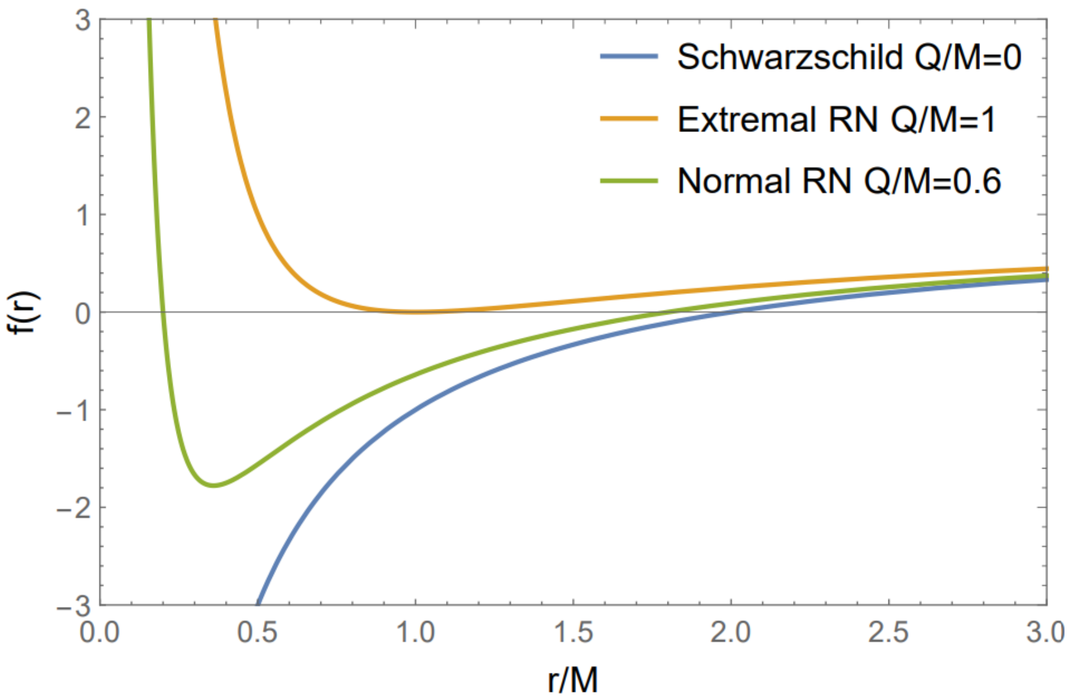

Fig. 2.2 – the function of f(r) for RN metric

The graph illustrates the metric function $f(r)$ of the Reissner-Nordström (RN) black hole for three different charge-to-mass ratios, namely Schwarzschild ($Q/M = 0$), non-extremal RN ($Q/M = 0.6$), and extremal RN ($Q/M = 1$). The Schwarzschild solution exhibits a single event horizon where $f(r) = 0$. For the non-extremal RN black hole, the function intersects the horizontal axis at two distinct points, corresponding to the inner and outer horizons. In the extremal case, these two horizons coincide, producing a degenerate horizon at $r = M$, where the curve is tangent to the axis. The figure clearly shows that increasing the electric charge modifies the behavior of $f(r)$ and significantly affects the horizon structure and spacetime geometry of the black hole.

2.3 Dark Matter

Dark matter constitutes an important component of the total energy density of the universe, representing about 23%, while ordinary baryonic matter represents only about 4%. Although it has not been directly detected, its existence is strongly supported by a wide range of astronomical observations, including the rotation curves of spiral galaxies, gravitational lensing, and large-scale cosmic structure. In particular, the flattening of the observed galaxy rotation curves cannot be explained by visible matter alone, indicating the presence of an additional non-luminous mass component. To describe the gravitational effects of dark matter, several theoretical models have been developed. Among them, the Perfect Fluid Dark Matter (PFDM) model, proposed by Kiselev [11], provides an effective framework in which dark matter is treated as an ideal fluid characterized by equal energy density and pressure. This approach allows for the integration of dark matter into spacetime geometry in a relatively simple and manageable way. The PFDM model has been widely applied to investigate the effect of dark matter on black hole spacetimes. In this context, it modifies the background geometry and thus affects the motion of test particles and photons. These modifications can lead to noticeable effects, including changes in gravitational lensing and frequency shifts of radiation emitted near black holes.

2.3.1 Evidence for Dark Matter

the Coma Cluster

The existence of dark matter was first proposed in the context of trying to explain the apparent discrepancy between the observed baryonic mass and the gravitational force needed to bind the components of galaxy clusters. In the 1930s, Fritz Zwicky conducted a study on the Coma Cluster, where he used the virial theorem to estimate the total mass of the cluster based on the velocities of the galaxies within it. His results showed that the high velocities of these galaxies could not be explained by relying solely on the visible mass, as the baryonic matter represented by stars and gas does not provide enough gravitational force to maintain the cluster's cohesion. And if this were the only mass present, the cluster would have disintegrated due to the motion of its components. This contradiction between the inferred dynamic mass and the observed mass led to the conclusion of the existence of an additional invisible component, which Zwicky named "dark matter." It is characterized by not interacting electromagnetically, but it effectively contributes to generating the gravitational field. This discovery formed a starting point for a deeper understanding of the structure of the universe, as it became necessary to assume the existence of this unobserved component to explain many subsequent astronomical phenomena, such as the stability of galaxy clusters and the distribution of mass on cosmic scales [12].

Fig. 2.3 – The Coma Galaxy Cluster contains over a thousand visible galaxies

The Bullet Cluster Evidence

The Bullet Cluster is a prominent and crucial example for studying mass distribution in complex astronomical systems. In this system, which consists of the collision of two galaxy clusters, a clear spatial separation occurs between the baryonic matter components. X-ray observations show that the hot gas (plasma), which constitutes the majority of the baryonic mass, experiences a noticeable slowdown due to pressure forces and hydrodynamic interactions during the collision, resulting in its displacement from its original position [12]. Galaxies move as nearly collisional systems through the collision zone with relatively limited interaction due to their small cross-section for direct interaction. Moreover, gravitational lensing maps, which track the total mass distribution independently of electromagnetic radiation, show that most of the mass is concentrated in regions corresponding to the locations of galaxies rather than the displaced gas.

Gravitational Lensing Results

Using gravitational lensing techniques, it is possible to reconstruct the total mass distribution of astronomical systems independently of their luminous components. In the case of the Bullet Cluster, lensing observations reveal that gravity is primarily concentrated around the distribution of galaxies rather than the X-ray-emitting plasma, which constitutes the bulk of the baryonic matter. This spatial offset between the peaks of the gravitational mass and the baryonic gas provides compelling evidence for the existence of a non-luminous and collisionless component. Such behavior is naturally explained within the dark matter model, where the main mass component interacts primarily through gravity and remains largely unaffected during the cluster collision. Therefore, these observations provide strong experimental support for the existence of dark matter and pose significant challenges to alternatives [12].

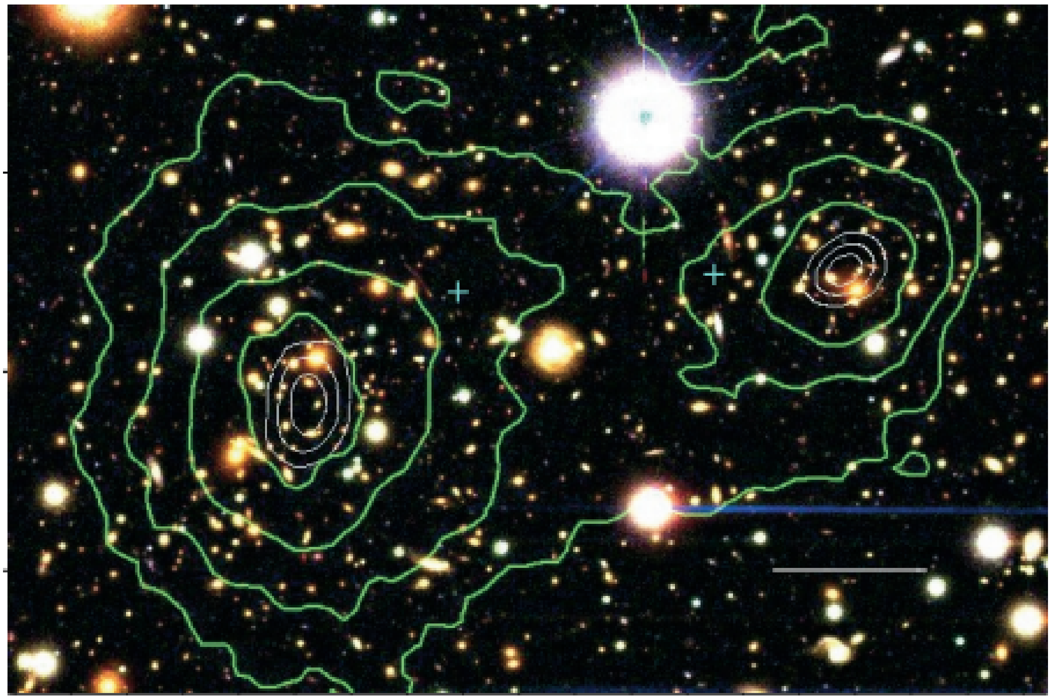

Fig. 2.4 – The Bullet Cluster from the Chandra Observatory with gravitational lensing maps

2.3.2 Dark Matter Models

The nature of dark matter still represents one of the most significant unresolved issues in modern cosmology and astrophysics, as its existence is not directly observed but is exclusively inferred from its gravitational effects on visible matter and light. Due to this indirect nature, a wide range of theoretical models have emerged aimed at describing its physical properties and cosmic distribution, from small galactic scales to large cosmic scales.

Alternative Theories

Several alternative approaches have been proposed to address this discrepancy, the most notable of which are modifications to gravitational dynamics such as Modified Newtonian Dynamics (MOND). These theories aim to reproduce the observed behavior of galaxies without resorting to an additional invisible mass component, by modifying the laws of gravity in low-acceleration systems. While these models have achieved notable success in explaining certain phenomena on the galactic scale—especially the flat rotation curves of spiral galaxies—they often rely on simplified assumptions, including ideal symmetry and dynamic equilibrium conditions. However, these assumptions limit their applicability when facing more complex astronomical physical systems, such as galaxy clusters, gravitational lensing observations, and cosmic data from the cosmic microwave background [12].

Cold Dark Matter (CDM)

The Cold Dark Matter model assumes that dark matter consists of non-relativistic particles that interact weakly with baryonic matter and electromagnetic radiation,and thus do not absorb, emit, or reflect light. They cannot be directly observed, but are inferred only through their gravitational effects on visible objects. The low velocity of the particles plays a crucial role, as it allows the preservation of small density fluctuations in the early universe without being erased by free streaming, enabling these fluctuations to gradually grow under the influence of gravity. Within the framework of the standard cosmological model ΛCDM, Λ represents the cosmological constant, which is associated with dark energy responsible for the accelerated expansion of the universe. This model describes the evolution of the universe based on general relativity, dark matter, and dark energy, where cold dark matter plays a fundamental role in the formation of cosmic structures on all scales. The ΛCDM model successfully explains the expansion of the universe, the formation of galaxies, and the cosmic microwave background, making it the most consistent cosmological model with modern astronomical observations. The process of structure formation begins with the amplification of the initial density fluctuations, leading to the emergence of dense regions of dark matter that subsequently undergo gravitational collapse to form dark matter halos, which serve as the fundamental building blocks for galaxy formation [13].

Hot and Warm Dark Matter

Alternative scenarios to the Cold Dark Matter (CDM) paradigm include Hot Dark Matter (HDM) and Warm Dark Matter (WDM) models, which differ mainly in the typical velocities and thermal properties of the dark matter particles, and consequently in their impact on cosmic structure formation. In HDM models, dark matter consists of relativistic or nearly relativistic particles, such as light neutrinos in the early Universe. Due to their high thermal velocities, these particles undergo significant free streaming, which refers to the rapid motion of particles across space without being efficiently trapped by gravitational perturbations. As a result, density fluctuations below a characteristic scale are smoothed out before gravity can amplify them. This process erases small-scale perturbations and leads to a top-down structure formation scenario, in which large-scale structures form first and later fragment into smaller systems. However, this prediction is in strong tension with astronomical observations indicating the early formation of small-scale structures such as galaxies. WDM represents an intermediate case between HDM and CDM, characterized by particles with moderate thermal velocities at the epoch of structure formation. These velocities are sufficient to suppress the growth of small-scale density perturbations through partial free streaming, while still allowing the formation of large-scale structures [18].

weakly interacting massive Particles

From the perspective of particle physics, several candidates for dark matter have been proposed, including weakly interacting massive particles (WIMPs), axions [14], and sterile neutrinos. These candidates naturally appear in various extensions of the Standard Model, such as supersymmetry, the Peccei-Quinn theory, and neutrino mass models that go beyond the Standard Model. WIMP particles are among the most studied candidates due to their natural production mechanism in the early universe through thermal freeze-out, which can lead to an abundance consistent with cosmic observations. Axions, originally proposed to solve the strong CP problem in quantum chromodynamics (QCD), are very light particles with weak interactions, and they can be produced non-thermally through vacuum misalignment and may constitute cold dark matter. On the other hand, sterile neutrinos are right-handed neutrino states that do not interact via the standard model forces, and they can contribute to dark matter either as warm or cold components depending on their mass and production mechanism.

2.3.3 Perfect Fluid Dark Matter (PFDM)

Perfect Fluid Dark Matter is a phenomenological framework in which dark matter is modeled not as a collection of discrete particles, but as an effective relativistic perfect fluid. Within this description, the dark matter component is characterized by macroscopic thermodynamic quantities such as energy density and pressure, rather than microscopic particle properties. In this approach, the influence of dark matter on spacetime is encoded through its energy–momentum tensor in the form of a perfect fluid, which is directly coupled to the Einstein field equations. Consequently, the gravitational effects of dark matter emerge from its fluid-like distribution, which modifies the spacetime geometry in a continuous manner. This formulation provides an effective description of dark matter on astrophysical and cosmological scales.
Equation of State
In general relativity, a perfect fluid is described by the energy-momentum tensor:

$$T_{\mu\nu}^{(PFDM)} = (\rho + p_t)u_\mu u_\nu + p_t g_{\mu\nu} + (p_r - p_t)\chi_\mu \chi_\nu, \tag{2.64}$$

where ρ is the energy density, p the pressure, and u_μ the four-velocity of the fluid.

PFDM in Black Hole Spacetimes

In the PFDM model, dark matter is treated as a continuous and ideal fluid instead of considering it as a collection of unknown particles. The microscopic nature of dark matter is ignored, and the focus is on macroscopic physical quantities such as density and pressure. These quantities directly enter the energy-momentum tensor within Einstein's equations, allowing for the representation of dark matter's effect on the curvature of spacetime. This framework also provides the possibility to study the effect of dark matter on both galactic scales and compact objects such as black holes. The inclusion of a PFDM background leads to systematic modifications of the gravitational field and its associated physical properties. In particular, it alters the effective gravitational potential, thereby influencing the dynamics of both massive and massless test particles through changes in the geodesic structure. Moreover, the presence of such a fluid component can significantly affect the horizon structure of compact objects, potentially modifying their locations and stability properties in comparison with standard vacuum solutions. These effects are especially relevant in the context of classical black hole geometries. For example, when applied to the RN spacetime, the PFDM contribution induces deviations from the conventional charged black hole solution, reflecting the impact of an ambient dark matter distribution on the causal structure and observable characteristics of the system.

Chapter 3

Charged Black Hole Dark Matter

The study of charged black holes is essential for understanding the interaction between gravitation and electromagnetic fields in general relativity. A fundamental solution in this context is the RN spacetime, which describes a static and spherically symmetric black hole endowed with electric charge. Unlike the Schwarzschild case, the presence of charge leads to a richer spacetime structure, including the existence of two horizons and a more complex causal behavior [6].

In order to obtain a more realistic description of astrophysical environments, it is important to consider the influence of surrounding dark matter distributions. One such approach is provided by Perfect Fluid Dark Matter , which models dark matter as a continuous perfect fluid characterized by its energy density and pressure. Embedding this model into the RN geometry leads to modifications of the spacetime metric and affects key properties such as the gravitational potential, horizon structure, and curvature behavior.

Moreover, observable phenomena such as gravitational redshift and blueshift offer valuable insights into the effects of spacetime curvature and the presence of dark matter. In this chapter, we investigate the RN black hole in a PFDM background by deriving the modified metric and analyzing its physical properties. Particular attention is given to horizon structure, singularity behavior, and frequency shifts in order to understand how dark matter influences the geometry and observable features of charged black holes [15].

3.1 Reissner–Nordström Black Hole Immersed in Perfect Fluid Dark Matter

The inclusion of PFDM significantly alters the characteristics of the classical RN black hole. Specifically, the presence of PFDM introduces a non-negligible contribution to the spacetime geometry, resulting in a metric that deviates from the asymptotically flat condition typically associated with these black holes. This deviation implies that the gravitational potential is affected at considerable distances due to the surrounding distribution of dark matter, fundamentally modifying the far-field behavior of the black hole's gravitational influence [19].

Metric

The PFDM RN metric is written in the form:

$$ds^2 = -f(r)\, dt^2 + \frac{1}{f(r)}\, dr^2 + r^2 \left(d\theta^2 + \sin^2\theta\, d\phi^2\right), \tag{3.1}$$

where the metric function is generalized as

$$f(r) = 1 - \frac{2M}{r} + \frac{Q^2}{r^2} + \frac{\alpha}{r} \ln\left(\frac{r}{|\alpha|}\right), \tag{3.2}$$

where M is the black hole mass, Q the electric charge, and α the PFDM parameter characterizing the density of the perfect fluid dark matter. The additional logarithmic term arises from solving Einstein's field equations with a perfect fluid dark matter energy–momentum tensor, and it encodes the long-range influence of the dark matter halo on the black hole geometry. This modification leads to significant changes in the horizon structure, geodesic motion, and thermodynamic properties compared to the standard RN solution.

Event Horizons

In the presence of PFDM, the horizon structure of the RN black hole is determined by the roots of the metric function

$$\begin{aligned} g^{rr} &= 0 \\ f(r) = 1 - \frac{2M}{r} + \frac{Q^2}{r^2} + \frac{\alpha}{r} \ln\left(\frac{r}{|\alpha|}\right) &= 0\,, \\ = \frac{r^2 - 2Mr + Q^2 + \alpha r \ln\left(r/|\alpha|\right)}{r^2} &= 0 \\ \Rightarrow\ r^2 - 2Mr + Q^2 + \alpha r \ln\left(\frac{r}{|\alpha|}\right) &= 0 \end{aligned}$$

This type of equation cannot be solved explicitly analytically for r_H. Therefore, the expression of the horizon r_H are obtained using numerical methods only. Thus, PFDM introduces quantitative modifications to the horizon structure while preserving the qualitative behavior observed in the standard RN spacetime.

Singularity and Curvature Behavior

The Kretschmann scalar for the RN black hole immersed in PFDM is

$$\begin{aligned} K &= R_{\mu\nu\alpha\beta} R^{\mu\nu\alpha\beta}, \\ K &= \frac{4}{r^4}\left[12\left(M - \frac{Q^2}{r} + \frac{\alpha}{2}\left(1 - \ln\frac{r}{\alpha}\right)\right)^2 + \frac{8Q^4}{r^4} - \frac{8Q^2}{r^3}\left(M + \frac{\alpha}{2}\left(1 - \ln\frac{r}{\alpha}\right)\right) + \alpha^2\right]. \end{aligned}$$

At the singularity $r \to 0$, the Kretschmann scalar diverges $K \to \infty$, confirming the persistence of the central singularity of the black hole even in the presence of dark matter

$$r_{Sing} = 0 \tag{3.3}$$

In the vacuum limit, setting $\alpha = 0$ and $Q = 0$ reduces the expression to $K = 48M^2/r^6$, which corresponds to the Schwarzschild black hole case.

3.2 Derivation of the Reissner–Nordström Metric with Perfect Fluid

In this section, We will derive the modified RN metric by solving the Einstein field equations in the presence of both an electromagnetic field and PFDM.

We will follow the same steps we took in the previous chapter The first step is the spherical symmetric metric Ansatz, which can be written as

$$ds^2 = -e^{2\Phi(r)}dt^2 + e^{2\Lambda(r)}dr^2 + r^2 d\Omega^2, \tag{3.4}$$

where $d\Omega^2 = d\theta^2 + \sin^2\theta\, d\phi^2$. Then we have the metric components

$$g_{tt} = -e^{2\Phi(r)}, \quad g_{rr} = e^{2\Lambda(r)}, \quad g_{\theta\theta} = r^2, \quad g_{\phi\phi} = r^2 \sin^2\theta\,, \tag{3.5}$$

and the inverse metric components:

$$g^{tt} = -e^{-2\Phi}, \quad g^{rr} = e^{-2\Lambda}, \quad g^{\theta\theta} = \frac{1}{r^2}, \quad g^{\phi\phi} = \frac{1}{r^2\sin^2\theta}. \tag{3.6}$$

The second step is to calculate the Christoffel symbols :

$$\begin{aligned}
&\Gamma^t_{tr} = \Phi'(r), && \Gamma^r_{tt} = e^{2(\Phi-\Lambda)}\Phi'(r), && \Gamma^r_{rr} = \Lambda'(r),\\
&\Gamma^r_{\theta\theta} = -re^{-2\Lambda}, && \Gamma^r_{\phi\phi} = -r\sin^2\theta\, e^{-2\Lambda} && \Gamma^\theta_{r\theta} = \Gamma^\phi_{r\phi} = \frac{1}{r}.
\end{aligned}$$

The third step is the Ricci tensor:

$$R_{\mu\nu} = \partial_\alpha \Gamma^\alpha_{\mu\nu} - \partial_\nu \Gamma^\alpha_{\mu\alpha} + \Gamma^\alpha_{\beta\alpha}\Gamma^\beta_{\mu\nu} - \Gamma^\alpha_{\beta\nu}\Gamma^\beta_{\mu\alpha}. \tag{3.7}$$

Following the same procedure as the previous chapter, we obtain

$$R_{tt} = e^{2(\Phi-\Lambda)}\left[\Phi'' + \Phi'^2 - \Phi'\Lambda' + \frac{2}{r}\Phi'\right], \tag{3.8}$$

$$R_{rr} = -\Phi'' - \Phi'^2 + \Phi'\Lambda' + \frac{2}{r}\Lambda', \tag{3.9}$$

$$R_{\theta\theta} = 1 - e^{-2\Lambda}(1 - r\Lambda' + r\Phi'), \tag{3.10}$$

$$R_{\phi\phi} = \sin^2\theta\,\left[1 - e^{-2\Lambda}(1 - r\Lambda' + r\Phi')\right] = \sin^2\theta\, R_{\theta\theta}. \tag{3.11}$$

The fourth step The Ricci scalar:

$$\begin{aligned}
R &= g^{\mu\nu}R_{\mu\nu} = g^{tt}R_{tt} + g^{rr}R_{rr} + g^{\theta\theta}R_{\theta\theta} + g^{\phi\phi}R_{\phi\phi},\\
&= \frac{2}{r^2}(1 - e^{-2\Lambda}) + e^{-2\Lambda}\left[-2\Phi'' - 2\Phi'^2 + 2\Phi'\Lambda' + \frac{4}{r}(\Lambda' - \Phi')\right].
\end{aligned} \tag{3.12}$$

By dividing the equations(3.8)and(3.9) by $g_{\mu\nu}$, we obtain

$$\begin{aligned}
\frac{R_{tt} - \frac{1}{2}g_{tt}R}{g_{tt}} &= -\frac{R_{rr} - \frac{1}{2}g_{rr}R}{g_{rr}},\\
\frac{R_{tt}}{g_{tt}} - \frac{1}{2}R &= -\frac{R_{rr}}{g_{rr}} - \frac{1}{2}R,\\
\frac{R_{tt}}{g_{tt}} &= -\frac{R_{rr}}{g_{rr}},\\
R_{tt}e^{-2\Phi} &= -R_{rr}e^{-2\Lambda}.
\end{aligned}$$

Following the same steps as in the previous chapter, we get

$$\Phi = -\Lambda. \tag{3.13}$$

By substituting this result in (3.10), we obtain

$$R_{\theta\theta} = 1 - e^{-2\Lambda} + 2r\Lambda' e^{-2\Lambda}.$$

By substituting (3.13) in (3.12), the Ricci scalar becomes

$$R = \frac{2}{r^2}(1 - e^{-2\Lambda}) + e^{-2\Lambda}\left[2\Lambda'' - 4\Lambda'^2 + \frac{8}{r}(\Lambda')\right].$$

The fifth step is to calculate the energy-momentum tensor. In this case, the energy-momentum tensor corresponding to both the electromagnetic (EM) field and the PFDM distribution surrounding the black hole.

$$T_{\mu\nu} = T_{\mu\nu}^{(EM)} + T_{\mu\nu}^{(PFDM)} \tag{3.14}$$

From the previous chapter the energy-momentum tensor of the EM field is given by

$$T_{tt}^{(EM)} = \frac{Q^2}{8\pi r^4} g_{tt} \tag{3.15a}$$
$$T_{rr}^{(EM)} = -\frac{Q^2}{8\pi r^4} g_{rr} \tag{3.15b}$$
$$T_{\theta\theta}^{(EM)} = \frac{Q^2}{8\pi r^4} g_{\theta\theta} \tag{3.15c}$$
$$T_{\phi\phi}^{(EM)} = \frac{Q^2}{8\pi r^4} g_{\phi\phi} \tag{3.15d}$$

the energy-momentum tensor for an anisotropic fluid

$$T_{\mu\nu}^{(PFDM)} = (\rho + p_t)u_\mu u_\nu + p_t g_{\mu\nu} + (p_r - p_t)\chi_\mu \chi_\nu \tag{3.16}$$

where

- u_μ is the fluid four-velocity vector,
- χ_μ is the radial unite vector,
- ρ is the energy density of the fluid,
- p_r is the radial pressure along the direction of χ_μ,
- p_t is the tangential (transverse) pressure orthogonal to χ_μ .

Using the metric given in (3.5), the expressions of these quantities are given by

$$u_\mu(r) = \left(-e^{-\Lambda(r)}, 0, 0, 0\right), \tag{3.17a}$$
$$\chi_\mu(r) = \left(0, e^{-\Lambda(r)}, 0, 0\right), \tag{3.17b}$$
$$\rho(r) = \frac{\alpha}{8\pi r^3}, \tag{3.17c}$$
$$p_r(r) = -\rho = -\frac{\alpha}{8\pi r^3}, \tag{3.17d}$$
$$P_t(r) = \frac{\rho}{2} = \frac{\alpha}{16\pi r^3}. \tag{3.17e}$$

Inserting these expressions in equation (3.16), get the energy-momentum tensor of the PFDM with the metric (3.5)

$$T_{tt}^{(PFDM)} = \rho\, e^{-2\Lambda(r)} = \frac{\alpha}{8\pi r^3} e^{-2\Lambda(r)} \tag{3.18a}$$
$$T_{rr}^{(PFDM)} = p_r\, e^{2\Lambda(r)} = -\frac{\alpha}{8\pi r^3} e^{2\Lambda(r)} \tag{3.18b}$$
$$T_{\theta\theta}^{(PFDM)} = p_t\, r^2 = \frac{\alpha}{16\pi r^3} r^2 \tag{3.18c}$$
$$T_{\phi\phi}^{(PFDM)} = p_t\, r^2 \sin^2\theta = \frac{\alpha}{16\pi r^3} r^2 \sin^2\theta \tag{3.18d}$$

Combining equations (3.15) and (3.18), the total energy-momentum tensor is

$$T_{\mu\nu} = T_{\mu\nu}^{(EM)} + T_{\mu\nu}^{(PFDM)} \tag{3.19a}$$
$$T_{tt} = \frac{Q^2}{8\pi r^4}(-e^{-2\Lambda(r)}) + \frac{\alpha}{8\pi r^3} e^{-2\Lambda(r)} = \frac{e^{-2\Lambda(r)}}{8\pi r^4}\left(-Q^2 + \alpha r\right), \tag{3.19b}$$
$$T_{rr} = -\frac{Q^2}{8\pi r^4} e^{2\Lambda(r)} - \frac{\alpha}{8\pi r^3} e^{2\Lambda(r)} = -\frac{e^{2\Lambda(r)}}{8\pi r^4}\left(Q^2 + \alpha r\right), \tag{3.19c}$$
$$T_{\theta\theta} = \frac{Q^2}{8\pi r^4} r^2 + \frac{\alpha}{16\pi r^3} r^2 = \frac{2Q^2 + \alpha r}{16\pi r^2}, \tag{3.19d}$$
$$T_{\phi\phi} = \frac{Q^2}{8\pi r^4} r^2 \sin^2\theta + \frac{\alpha}{16\pi r^3} r^2 \sin^2\theta = \frac{\sin^2\theta}{16\pi r^2}(2Q^2 + \alpha r). \tag{3.19e}$$

The sixth step is to solve Einstein's equations coupled with both the electromagnetic field and the fluid as follows:

$$R_{\mu\nu} - \frac{1}{2} g_{\mu\nu} R = 8\pi\left(T_{\mu\nu}^{(EM)} + T_{\mu\nu}^{(PFDM)}\right) \tag{3.20}$$

Among these quations, the only independent ones are

$$R_{tt} - \frac{1}{2} g_{tt} R = \frac{e^{-2\Lambda(r)}}{r^4}\left(-Q^2 + \alpha r\right) \tag{3.21a}$$
$$R_{rr} - \frac{1}{2} g_{rr} R = -\frac{e^{2\Lambda(r)}}{r^4}\left(Q^2 + \alpha r\right) \tag{3.21b}$$
$$R_{\theta\theta} - \frac{1}{2} g_{\theta\theta} R = \frac{1}{r^2}(Q^2 + \alpha r), \tag{3.21c}$$
$$R_{\phi\phi} - \frac{1}{2} g_{\phi\phi} R = \frac{\sin^2\theta}{8r^2}(2Q^2 + \alpha r). \tag{3.21d}$$

Inserting $R_{\theta\theta}$, R and $T_{\theta\theta}$ in the $\theta\theta$ Einstein's equation, we get

$$R_{\theta\theta} - \frac{1}{2} g_{\theta\theta} R = \frac{Q^2 + \alpha r}{r^2},$$

As in the previous chapter, after simplification, we obtain this expression

$$r^2 e^{-2\Lambda}\left(-\Lambda'' + 2(\Lambda')^2 - \frac{2}{r}\Lambda'\right) = \frac{Q^2}{r^2} + \frac{\alpha}{2r}, \tag{3.22}$$

The left hand side of this equation can be written as

$$r^2 e^{-2\Lambda}\left[-\Lambda'' + 2(\Lambda')^2 - \frac{2}{r}\Lambda'\right] = \frac{r}{2}\frac{d^2}{dr^2}\left(re^{-2\Lambda}\right), \tag{3.23}$$

which allows as to integrate equation (3.22) as follows

$$\begin{aligned}
\frac{r}{2}\frac{d^2}{dr^2}\left(re^{-2\Lambda}\right) &= \frac{Q^2}{r^2}+\frac{\alpha}{2r} \\
\frac{d^2}{dr^2}\left(re^{-2\Lambda}\right) &= \frac{2Q^2}{r^3}+\frac{\alpha}{r^2} \\
\frac{d}{dr}\left(re^{-2\Lambda}\right) &= -\frac{Q^2}{r^2}+C_1+\frac{\alpha}{r} \\
re^{-2\Lambda} &= \frac{Q^2}{r}+C_1 r+\alpha\ln r+C_2 \\
e^{-2\Lambda} &= C_1+\frac{C_2}{r}+\frac{Q^2}{r^2}+\frac{\alpha}{r}\ln r,
\end{aligned}$$

where C_1 and C_2 are integration constants that can be identified Using the Newtonian limit $e^{-2\Lambda} \approx 1-\frac{2M}{r}$

$$f(r) = e^{-2\Lambda} \to 1-\frac{2M}{r}, \tag{3.24}$$

$$\Longrightarrow C_1 = 1\ , \quad C_2 = -2M, \tag{3.25}$$

$$e^{-2\Lambda} = 1-\frac{2M}{r}+\frac{Q^2}{r^2}-\frac{\alpha}{r}\ln r = f(r). \tag{3.26}$$

To make the logarithmic argument dimensionless, a parameter α having the same dimension as the argument r is introduced inside the logarithm. Therefore, the term is written as

$$\ln\left(\frac{r}{|\alpha|}\right).$$

Finally, the expression of the metric of the RN black hole immersed in PFDM is

$$ds^2 = -\left(1-\frac{2M}{r}+\frac{Q^2}{r^2}-\frac{\alpha}{r}\ln\left(\frac{r}{|\alpha|}\right)\right)dt^2+\left(1-\frac{2M}{r}+\frac{Q^2}{r^2}-\frac{\alpha}{r}\ln\left(\frac{r}{|\alpha|}\right)\right)^{-1}dr^2+r^2d\Omega^2. \tag{3.27}$$

In the image(3.1), we plotted the function $f(r)$ with respect to r for three values of $\frac{\alpha}{M} = (0, 0.7, 0.5)$ with take a fixed value of ($\frac{Q}{M} = 0.6$),we obtain

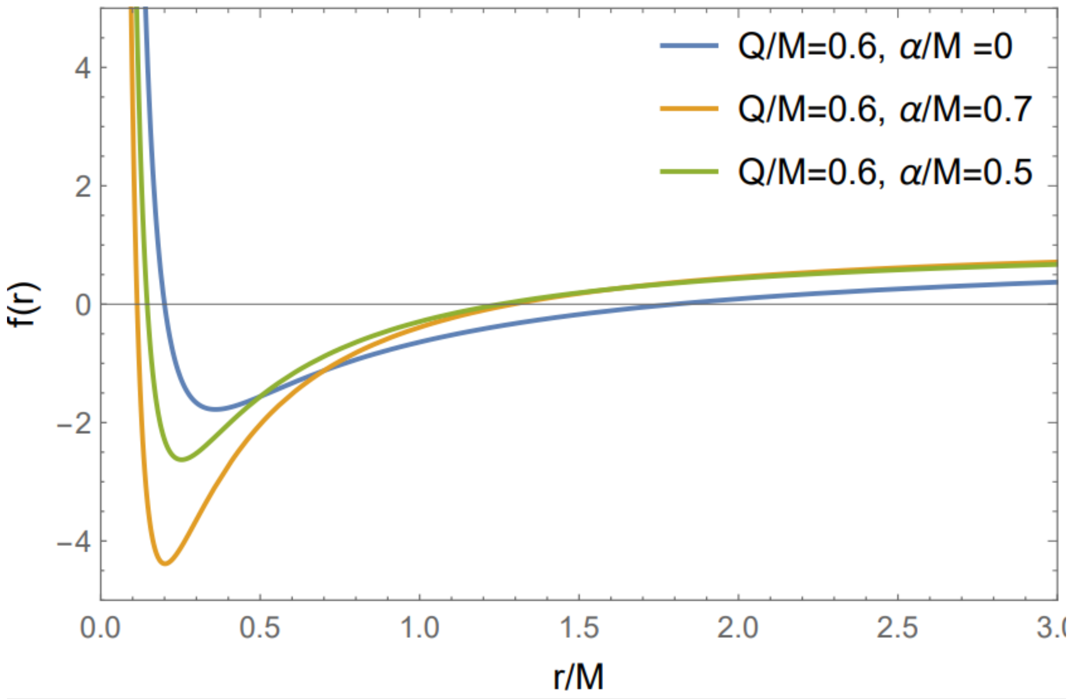

Fig. 3.1 – the function of f(r) for RN metric with PFDM

The graph shows the metric function $f(r)$ for a Reissner–Nordström black hole surrounded by Perfect Fluid Dark Matter (PFDM), with a fixed charge-to-mass ratio $Q/M = 0.6$ and three different values of the PFDM parameter α/M. The blue curve ($\alpha/M = 0$) corresponds to the standard RN black hole without dark matter, while the green ($\alpha/M = 0.5$) and orange ($\alpha/M = 0.7$) curves represent increasing PFDM contributions. As α increases, the minimum of $f(r)$ becomes deeper and shifts slightly, indicating a stronger influence of dark matter on the spacetime geometry. The presence of PFDM modifies the horizon structure and the behavior of the metric function, particularly in the region close to the black hole, while all curves approach positive values at large distances. This demonstrates that the PFDM parameter plays an important role in shaping the gravitational field around the charged black hole.

3.3 Circular Orbits and Expression of r_{ISCO}

Since we are interested in circular orbits, we restrict the motion to the equatorial plane without loss of generality [15]. Thus, we set

$$\theta = \frac{\pi}{2}, \quad U^\theta = 0.$$

The four-velocity of massive particles satisfies the normalization condition

$$U^\mu U_\mu = -1.$$

Using the spacetime metric introduced above, this condition becomes:

$$-1 = -f(r)(U^t)^2 + \frac{1}{f(r)}(U^r)^2 + r^2(U^\phi)^2. \tag{3.28}$$

In a stationary and spherically symmetric spacetime, Killing symmetries give rise to conserved energy and angular momentum.

The spacetime admits two Killing vectors associated with its symmetries:

$$\xi^\mu = (1, 0, 0, 0), \quad \text{(time translation symmetry)} \tag{3.29}$$

$$\psi^\mu = (0, 0, 0, 1). \quad \text{(axial symmetry)} \tag{3.30}$$

Using the Killing vectors, the conserved quantities along geodesics are defined as:

$$E = -\xi_\mu U^\mu = f(r)\, U^t, \tag{3.31}$$

$$L = \psi_\mu U^\mu = r^2 \sin^2\theta\, U^\phi = r^2\, U^\phi. \tag{3.32}$$

Thus, we obtain

$$U^t = \frac{E}{f(r)}, \tag{3.33}$$

$$U^\phi = \frac{L}{r^2}. \tag{3.34}$$

Using the normalization condition $U^\mu U_\mu = -1$,we compensate U^t and U^ϕ in (3.28):

$$-1 = -\frac{E^2}{f(r)} + \frac{(U^r)^2}{f(r)} + \frac{L^2}{r^2}, \tag{3.35}$$

$$-f(r) = -E^2 + (U^r)^2 + \frac{f(r)L^2}{r^2}. \tag{3.36}$$

The equation of motion for a particle moving in an orbit around a black hole [15]:

$$(U^r)^2 = E^2 - f(r)\left(1 + \frac{L^2}{r^2}\right), \tag{3.37}$$

$$= E^2 - V_{\text{eff}}(r), \tag{3.38}$$

where

$$V_{\text{eff}}(r) = f(r)\left(1 + \frac{L^2}{r^2}\right). \tag{3.39}$$

By substituting in the RN metric with (PFDM) (3.26):

$$V_{\text{eff}}(r) = \frac{1}{2}\left[\left(1 - \frac{2M}{r} + \frac{Q^2}{r^2} - \frac{\alpha}{r}\ln r\right)\left(1 + \frac{L^2}{r^2}\right)\right]. \tag{3.40}$$

The conditions for circular orbits are obtained by requiring that the effective potential equals the square of the conserved energy, $V_{\text{eff}}(r) = E^2$. In addition, the stability of the orbit requires that the radial derivative of the effective potential vanishes, $\frac{dV_{\text{eff}}(r)}{dr} = 0$.

$$\frac{dV_{\text{eff}}}{dr} = \frac{1}{2}\left[\frac{2M}{r^2} - \frac{2Q^2}{r^3} + \alpha\frac{1 - \ln r}{r^2} - \frac{2L^2}{r^3} + \frac{6ML^2}{r^4} - \frac{4Q^2L^2}{r^5} + \alpha L^2\frac{1 - 3\ln r}{r^4}\right] = 0. \tag{3.41}$$

By solving this system of equations, we obtain general expressions for the conserved energy E and angular momentum L in terms of the metric function $f(r)$.
First calculate the angular momentum of a circular orbit L^2:
we have the circular orbit condition

$$E^2 = V_{\text{eff}}(r) \;\Rightarrow\; E^2 = f(r)\left(1 + \frac{L^2}{r^2}\right), \tag{3.42}$$

and:

$$V'_{\text{eff}}(r) = 0. \tag{3.43}$$

starting from the effective potential (3.39) differentiating with respect to r,we obtain

$$f'(r)\left(1+\frac{L^2}{r^2}\right) - \frac{2L^2}{r^3}f(r) = 0, \tag{3.44}$$

$$f'(r) + \frac{L^2 f'(r)}{r^2} - \frac{2L^2 f(r)}{r^3} = 0, \tag{3.45}$$

$$L^2\left(\frac{f'(r)}{r^2} - \frac{2f(r)}{r^3}\right) = -f'(r), \tag{3.46}$$

$$L^2(rf'(r) - 2f(r)) = -r^3 f'(r). \tag{3.47}$$

So, the expression of the angular momentum of a circular orbit is:

$$L^2(r) = \frac{r^3 f'(r)}{2f(r) - rf'(r)}. \tag{3.48}$$

Second the expression of E^2:
by substituting the value of L^2 in the expression (3.42):

$$E^2 = f(r)\left(1 + \frac{rf'(r)}{2f(r) - rf'(r)}\right), \tag{3.49}$$

$$E^2 = f(r)\left(\frac{2f(r) - rf'(r) + rf'(r)}{2f(r) - rf'(r)}\right), \tag{3.50}$$

$$E^2 = f(r)\left(\frac{2f(r)}{2f(r) - rf'(r)}\right). \tag{3.51}$$

So, the expression for the energy of the circular orbit is:

$$E^2(r) = \frac{2[f(r)]^2}{2f(r) - rf'(r)}. \tag{3.52}$$

The metric is:

$$f(r) = 1 - \frac{2M}{r} + \frac{Q^2}{r^2} + \frac{\gamma}{r}\, ln\left(\frac{r}{\gamma}\right). \tag{3.53}$$

We know that the derivative of the metric is :

$$f'(r) = \frac{2M}{r^2} - \frac{2Q^2}{r^3} - \frac{\gamma\left[1 + \ln\left(\frac{\gamma}{r}\right)\right]}{r^2}. \tag{3.54}$$

By substituting the expression (3.54) in (3.48) and (3.52), we obtain:

$$L^2 = \frac{2Mr - 2Q^2 - \gamma r\left[1 + \ln\left(\frac{\gamma}{r}\right)\right]}{2 - \frac{6M}{r} + \frac{4Q^2}{r^2} + \frac{\gamma\left[1+3\ln\left(\frac{\gamma}{r}\right)\right]}{r}}, \tag{3.55}$$

$$E^2 = \frac{2\left[1 - \frac{2M}{r} + \frac{Q^2}{r^2} + \frac{\gamma}{r}\ln\left(\frac{\gamma}{r}\right)\right]^2}{2 - \frac{6M}{r} + \frac{4Q^2}{r^2} + \frac{\gamma\left[1+3\ln\left(\frac{\gamma}{r}\right)\right]}{r}}. \tag{3.56}$$

This condition defines the allowed physical domain for the motion of the particle around the black hole, ensuring that the particle's energy E is real (not imaginary). That is, it determines the values of the radius r that allow for the existence of stable or possible physical orbits.

$$r(-\gamma - 6M + 2r) + 4Q^2 + 3\gamma r \ln\left(\frac{r}{\gamma}\right) > 0.$$

Schwarzschild limit: If we set $Q = 0$ and $\gamma = 0$, the equations reduce to the well-known classical result ($L^2 = \frac{Mr}{1-3M/r}$).

Dark matter effect (γ): The parameter γ appears in both the numerator and denominator. Its presence in the numerator indicates a direct contribution to increasing the angular momentum required for a stable circular orbit.

Stability Circular orbits exist only when the denominator is positive. The presence of dark matter modifies the critical values of the radius r that allows stable orbital motion.

In order to determine the stability of circular orbits around the black hole, we analyze the effective potential governing particle motion. The innermost stable circular orbit (ISCO) is obtained by imposing the condition that the second derivative of the effective potential satisfies it.

$$V''_{\text{eff}}(r) = 0.$$

There exists a compact relation linking the second derivative of the effective potential $V''_{\text{eff}}(r)$ to the metric function $f(r)$ at circular orbits.

$$V''_{\text{eff}}(r) > 0 \quad \Rightarrow \quad \text{Stable circular orbit,}$$

$$V''_{\text{eff}}(r) < 0 \quad \Rightarrow \quad \text{Unstable circular orbit.}$$

For the orbit to be stable, it must be

$$f(r)\,[3f'(r) + rf''(r)] - 2r[f'(r)]^2 \geq 0. \tag{3.57}$$

We derive the equation (3.54) again we get:

$$f''(r) = -\frac{4M}{r^3} + \frac{6Q^2}{r^4} + \frac{\gamma\left[1 + 2\ln\left(\frac{\gamma}{r}\right)\right]}{r^3}. \tag{3.58}$$

The expression of the U^t and U^ϕ:

The time component U^t expresses the relationship between the "coordinate time" and the "proper time" of the particle [15].

$$U^t = \sqrt{\frac{2r^2}{r(-\gamma - 6M + 2r) + 4Q^2 + 3\gamma r \ln\left(\frac{r}{\gamma}\right)}}. \tag{3.59}$$

- In Orbital Motion Calculation U^t serves as the key to determining the angular velocity $\Omega = \frac{U^\phi}{U^t}$,transforming the particle's proper time into the coordinate time of a distant observer.

- In Orbital Stability Study
  U^t is essential for defining the conserved energy of the particle $E = -g_{tt}U^t$, which directly constructs the effective potential $V_{eff}(r)$ used to locate the ISCO.

- In Near-Horizon Particle Analysis
  The divergence of this component

$$(U^t \to \infty)$$

  physically marks the location of the event horizon r_+ , quantifying the extreme gravitational redshift.
  While the angular component U^ϕ expresses the angular velocity

$$U^\phi = \sqrt{\frac{r(\gamma + 2M) - 2Q^2 + \gamma r \ln\left(\frac{\gamma}{r}\right)}{r^2\left[r(-\gamma - 6M + 2r) + 4Q^2 + 3\gamma r \ln\left(\frac{r}{\gamma}\right)\right]}}. \tag{3.60}$$

- In Orbital Motion Calculation
  U^ϕ quantifies the physical rate of angular rotation $\frac{d\phi}{d\tau}$, which provides the necessary centrifugal counter-balance against the gravitational pull.

- In Orbital Stability Study
  U^ϕ is essential for defining the conserved angular momentum $L = g_{\phi\phi}U^\phi$,which determines the shape of the effective potential barrier $V_{eff}(r)$ and regulates orbit stability.

- In Near-Horizon Particle Analysis
  As the particle approaches the horizon, U^ϕ combined with U^t shows that the orbital speed relative to a local observer approaches the speed of light c, defining the absolute limit of circularity. **T**he ISCO equation in the presence of dark matter:
  We compute the radius of the Innermost Stable Circular Orbit , which represents the smallest stable circular orbit around the black hole. The circular orbit conditions are given by (3.39) and (3.41). In addition, the stability condition requires (3.57) at the critical point. By applying these conditions together with the previous equations, the ISCO radius (r_{ISCO}) can be determined.

$$\begin{aligned} & r^2 - 2\gamma^2 - 12M^2 - 8\gamma M + 12\gamma M \ln\left(\frac{r}{\gamma}\right) - 3\gamma^2 \ln^2\left(\frac{r}{\gamma}\right) \\ & \quad + 4\gamma^2 \ln\left(\frac{r}{\gamma}\right) + r\left[2Q^2(4\gamma + 9M) - 9\gamma Q^2 \ln\left(\frac{r}{\gamma}\right)\right] \\ & \quad + r^2\left[2M - \gamma \ln\left(\frac{r}{\gamma}\right)\right] - 8Q^4 = 0. \end{aligned} \tag{3.61}$$

Since the ISCO equation is highly nonlinear, it cannot be solved analytically, and thus numerical methods are used. The behavior of the ISCO radius r_{ISCO} is analyzed as a function of the electric charge Q for different values of the PFDM parameter γ. In the Schwarzschild limit, where $Q = 0$ and $\gamma = 0$, the standard result $r_{\mathrm{ISCO}} = 6M$ is recovered. However, when either the electric charge or the PFDM coefficient is non-zero, the ISCO radius becomes smaller than $6M$. In general, increasing Q leads to a decrease in r_{ISCO} for any fixed value of γ, and similarly, increasing γ also reduces r_{ISCO} for any given charge [19]. This behavior can be interpreted as the joint contribution of the electromagnetic field and the PFDM component in enhancing the curvature of spacetime through the energy-momentum tensor, which strengthens the gravitational field and allows for the existence of stable orbits near the black hole.

In the image(3.2), we plotted the r_{ISCO} with respect to Q for values of $\alpha = (0, 0.04, 0.1, 0.3)$, we obtain

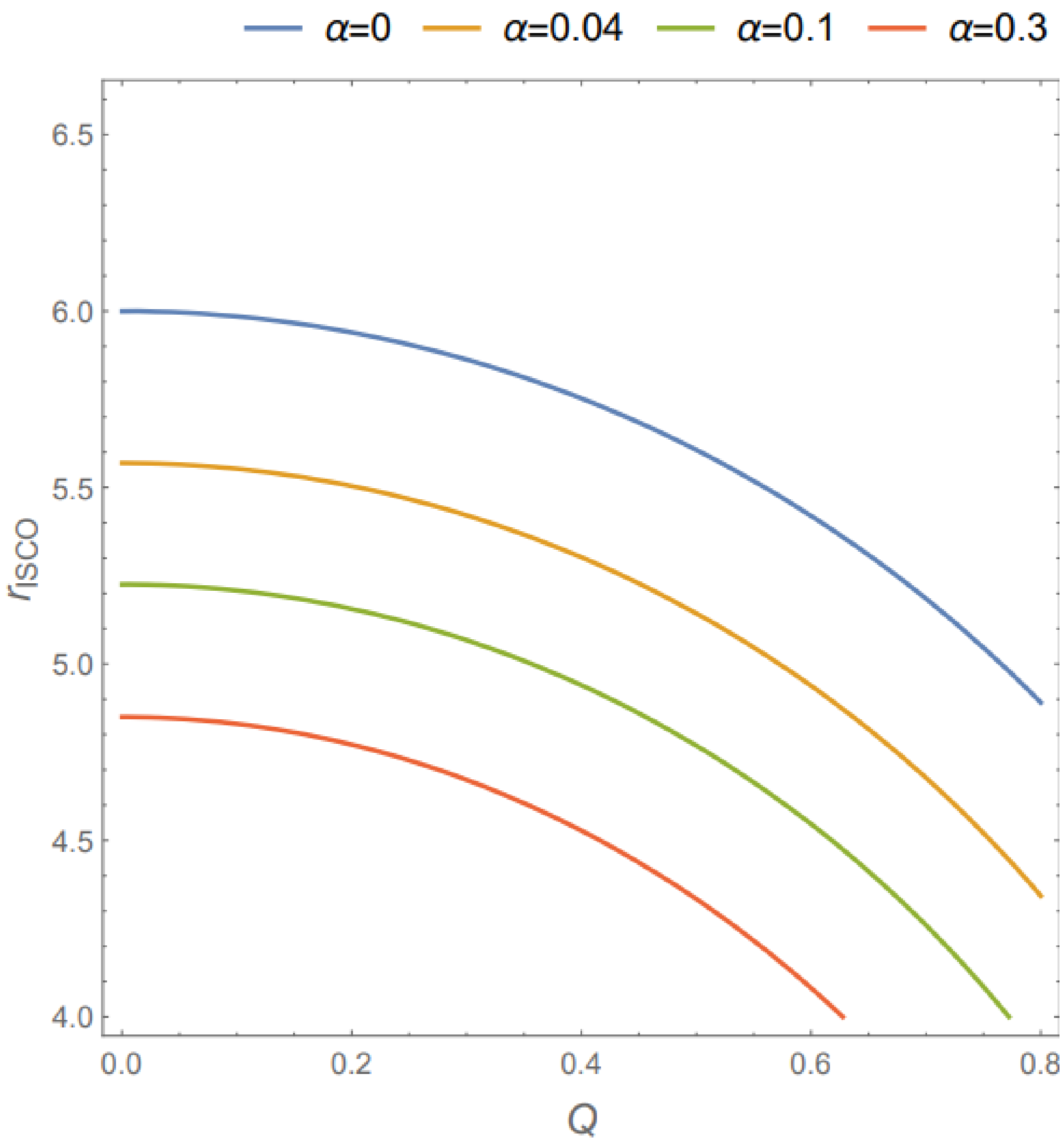

Fig. 3.2 – the r_{ISCO} of RN black hole immersed in PFDM

The figure illustrates the variation of the innermost stable circular orbit radius, r_{ISCO}, as a function of the black hole charge Q for several values of the PFDM parameter α. For all curves, r_{ISCO} decreases as the charge increases, indicating that stable circular orbits can exist closer to the black hole when the electric charge becomes larger. Moreover, increasing the PFDM parameter α shifts the curves downward, leading to smaller values of r_{ISCO} for a given charge. This behavior shows that both the electric charge and the surrounding perfect fluid dark matter influence the location of the innermost stable orbit. Therefore, the presence of PFDM enhances the gravitational effects near the black hole and allows stable particle motion at smaller orbital radii.

Conculusion

This work revolves around the study of black holes within the framework of general relativity [?], focusing on the RN black hole model surrounded by dark matter as a perfect fluid. The study began with a review of the foundational concepts of special [1] and general relativity that explain gravity as the curvature of spacetime governed by Einstein's field equations, followed by a comprehensive presentation of the properties of black holes [10] and their classical classifications (Schwarzschild, Kerr, and Kerr-Newman) based on the "no-hair" theorem. The focus of the research was on the effect of PFDM in modifying the spacetime metric of an RN black hole, where the new spacetime geometry was derived and analyzed, and the impact of dark matter on the structure of the event horizon [11] was demonstrated. The work also included a study of particle dynamics by determining circular orbits and the innermost stable circular orbit , demonstrating the role of the dark matter parameter in altering the stability of orbits and the motion of bodies in strong gravitational regions. The work concludes by providing a theoretical framework that enhances the understanding of black hole behavior in realistic astronomical environments that combine electromagnetic charge and dark matter effects.

Bibliography

[1] Tsamparlis, M. (2010). *Special Relativity.* Berlin: Springer.

[2] Rindler, W. (2001). Relativity: Special, general, and cosmological (2nd ed.). Oxford University Press.

[3] Daniell, A. (1925). The Michelson-Morley Experiment. Nature, 115(2889), 378-379.

[4] Schutz, B. F. (2009). A first course in general relativity (2nd ed.). Cambridge University Press.

[5] Carroll, S. M. (2019). An introduction to general relativity: Spacetime and geometry. Cambridge University Press.

[6] Hartle, J. B. (2021). Gravity: an introduction to Einstein's general relativity. Cambridge University Press.

[7] Wald, R. M. (2010). General relativity. University of Chicago press.

[8] Einstein, A. (2019). Relativity: The Special and the General Theories—100th Anniversary Edition.

[9] Nastase, H. (2019). General relativity: A graduate course. Cambridge University Press.

[10] Chandrasekhar, S. (1998). The mathematical theory of black holes (Vol. 69). Oxford University Press.

[11] Kiselev, V. (2003). Quintessence and black holes. Classical and Quantum Gravity, 20(6), 1187-1197.

[12] Clowe, D., Bradač, M., Gonzalez, A. H., Markevitch, M., Randall, S. W., Jones, C. Zaritsky, D. (2006). A direct empirical proof of the existence of dark matter. The Astrophysical Journal Letters, 648(2), L109-L113.

[13] Blumenthal, G. R., Faber, S. M., Primack, J. R. Rees, M. J. (1984). Formation of galaxies and large-scale structure with cold dark matter. Nature, 311(5986), 517-525.

[14] Wilczek, F. (1978). Problem of Strong P and T Invariance in the Presence of Instantons. Physical Review Letters, 40(5), 279.

[15] Trad, H. E. Khodja, L. (2025). Frequency Shift of Photons in Reissner-Nordström Black Hole Immersed in Perfect Fluid Dark Matter. International Journal of Theoretical Physics, 64(6), 160.

[16] Ryder, L. (2009). Introduction to general relativity. Cambridge University Press.

[17] Thorne, K. S., Misner, C. W. Wheeler, J. A. (2000). Gravitation. San Francisco: Freeman.

[18] Bond, J. R., Efstathiou, G.Silk, J. (1980). Massive neutrinos and the large-scale structure of the universe. Physical Review Letters, 45(24).

[19] Xu, Z., Hou, X., Wang, J.Liao, Y. (2019). Perfect Fluid Dark Matter Influence on Thermodynamics and Phase Transition for a Reissner-Nordstrom-Anti-de Sitter Black Hole. Advances in High Energy Physics, 2019(1), 2434390.